Running head:

ANCIENT MUDDY SUBAQUEOUS-DELTAIC CLINOFORMS

Title:

SEDIMENTOLOGIC CHARACTER OF ANCIENT MUDDY SUBAQUEOUS-DELTAIC CLINOFORMS: DOWN CLIFF CLAY MEMBER, BRIDPORT SAND FORMATION, WESSEX BASIN, UK

Authors:

GARY J. HAMPSON, KANOKKORN PREMWICHEIN[1]

Department of Earth Science and Engineering, Imperial College London, South Kensington Campus, London SW7 2AZ, UK.

[1]present address: PTTEP, Chatuchak, Bangkok 10900, Thailand.

E-mail:

g.j.hampson@imperial.ac.uk

Key words:

clinoform, subaqueous delta, mudstone, Bridport Sand Formation, Wessex Basin

Word count (abstract):	358
Word count (text):	7,152
Word count (references):	1,984
Word count (figure captions):	1,293
Number of figures:	9
Number of tables:	1

ABSTRACT

Muddy subaqueous clinoforms are a common feature of many modern deltas, particularly those developed in basins with strong waves, tides or oceanographic currents. Ancient examples have only rarely been reported, implying that they are under-recognised. Herein, the sedimentological characteristics of muddy subaqueous-deltaic clinoforms from the Lower Jurassic Down Cliff Clay Member of the Bridport Sand Formation, Wessex Basin, UK are described and interpreted, as a reference to re-evaluate other ancient shallow-marine mudstone successions.

Deposits below the Down Cliff Clay clinoforms consist of erosionally based, bioclastic sandy limestone beds intercalated with upward-thickening fossiliferous claystones and siltstones (facies association A), which record upward-increasing water depth under conditions of minor clastic sediment input and reworking by storm waves. These deposits are downlapped by foreset-to-toeset deposits of the subaqueous-deltaic clinoforms, which comprise claystones and siltstones that contain calcareous nodules and are variably bioturbated by a low-diversity trace fossil assemblages dominated by *Chondrites* (facies association B). These foreset-to-toeset deposits record slow deposition (undecompacted sediment accumulation rate of c. 4.4 m/Myr) from suspension fall-out and distal sediment gravity flows under conditions of intermittent and/or poor oxygenation of bottom waters. Clinoform foreset deposits dip paleoseaward at 2°, and consist of siltstones and sandy siltstones that are moderately to completely bioturbated by a high-diversity trace fossil assemblage (facies association C). Thin (<1 cm), erosionally based, parallel-laminated and current-ripple cross-laminated siltstone and very fine-grained sandstone beds in the foreset deposits record episodic sediment gravity flows and tractional currents. Foreset deposits record relatively rapid deposition (undecompacted sediment accumulation rate of c. 194 m/Myr) above effective storm wave base in well-oxygenated, fully marine bottom waters. Clinoform topset deposits comprise iron-stained and chloritic siltstones that contain iron-stained and phosphatic ooids, phosphatic pebbles, and fragmented and abraded body fossils (facies association D); these deposits record prolonged physical reworking, winnowing and sediment bypass. The long-term progradation rate of the subaqueous-deltaic clinoforms was c. 5.6 km/Myr (c. 6.7 km/Myr accounting for decompaction). The bed-scale sedimentologic characteristics of clinoform topsets, foresets and bottomsets are consistent with variations in sedimentation rate resolved in high-resolution biostratigraphic data and with seismic-geomorphic relationships, and provide criteria to aid identification of other subaqueous deltaic clinoforms in the stratigraphic record.

[end of abstract]

INTRODUCTION

Clinoforms are seaward-dipping stratal surfaces that characterise shoreface, delta-front and continental slopes (e.g. Rich 1951; Sangree and Widmier 1977). They have been widely documented and analysed in many modern and ancient examples of such settings, where they represent the dominant geomorphic landform and geometric stratal configuration, respectively. Many modern deltas have a compound clinoform morphology comprising an inner, subaerial clinoform with the shoreline at its topset-foreset break and an outer, subaqueous clinoform (Fig. 1) (e.g. Ganges-Brahmaputra Delta, Michels et al. 1998; Po Delta and western Adriatic shelf, Cattaneo et al. 2003, 2007; Yellow River Delta, Liu et al. 2004; Yangtze River Delta, Liu et al. 2006). The two clinoforms are separated by a broad subaqueous platform characterised by sediment erosion, transport and bypass due to high bed shear stress resulting from large storm waves and/or strong tidal currents (Fig. 1) (Pirmez et al. 1998; Driscoll and Karner 1999; Swenson et al. 2005; Mitchell et al. 2012).

Numerous examples of inner, subaerial deltaic clinoforms are described from ancient strata, but only a few examples of outer, subaqueous-deltaic clinoforms have been documented (Cretaceous "Kenilworth-Mancos Delta" and clinoforms in the Cody Shale, lower Pierre Shale, Tropic Shale, and Frontier Formation, Western Interior Basin, onshore USA, Asquith 1970; Leithold 1993, 1994; Vakarelov et al. 2005; Hampson 2010; Jurassic "Troll Delta", North Sea Basin, offshore Norway, Patruno et al. 2015a, 2015b). The apparent scarcity of ancient subaqueous-deltaic clinoforms may in part reflect the mud-prone character and low-angle dips of many such subaqueus deltaic clinoforms, as typified by modern deltas (e.g. Patruno et al. 2015b), which makes them difficult to identify in the absence of dense, high-quality data that allow stratal geometries to be resolved (e.g. high-resolution seismic data or continuous, well-exposed outcrops). However, it can also be partly attributed to a lack of diagnostic sedimentologic criteria for their recognition in ancient successions. Modern subaqueous-deltaic clinoforms are described from shallow cores that typically extend for only several metres below the surface (but in rare cases for several tens of metres; Sultan et al. 2008), and are characterized by thin (centimetre-scale) graded sand-silt beds, which contain cross-lamination and parallel lamination, intercalated with variably bioturbated, laminated silt-clay intervals (e.g. Michels et al. 1998; Cattaneo et al. 2003, 2007; Liu et al. 2004, 2006). Short-term (<100 yr) sediment accumulation rates have been measured in these modern clinoforms using short-lived radionucleides (e.g. ^{210}Pb; Michels et al. 1998; Cattaneo et al. 2003, 2007; Liu et al. 2004, 2006), and in some instances reconstructed over longer periods (100s-1000s yr) by integration of radiocarbon age, paleomagnetic and/or shallow, high-resolution seismic data (Cattaneo et al. 2004; Vigliotti et al. 2008). Ancient subaqueous-deltaic clinoforms from the Cretaceous Western Interior Basin are described from weathered outcrops, and are composed of variably bioturbated and laminated claystones and siltstones with thin (1-2 cm), planar-laminated and current-ripple cross-laminated sandstone beds (Leithold 1993, 1994; Hampson 2010). Although the durations of the regressive-transgressive cycles that contain these clinoforms are constrained by ammonite biostratigraphy and radiometric dating of bentonites, the rates of sediment accumulation and progradation of the clinoforms are essentially unknown because individual clinoforms are not dated (e.g. such that the method of Patruno et al. 2015c cannot be applied).

In this paper, we document the sedimentologic character in continuous core data of ancient muddy subaqueous-deltaic clinoforms that are recognised in seismic data on the basis of their geometric stratal configuration, using data from a shallow intracratonic seaway (Wessex Basin, onshore UK). The aims of the paper are threefold: (1) to describe the detailed sedimentologic character of ancient subaqueous-deltaic clinoforms in the Lower Jurassic Down Cliff Clay Member of the Bridport Sand Formation, (2) to interpret the processes responsible for sediment transport and clinoform accumulation, and (3) to infer long-term clinoform progradation rate from biostratigraphic data. The Down Cliff Clay Member clinoforms provide a reference with which the stratal geometries of other ancient shallow-marine mudstone successions can be re-evaluated.

GEOLOGIC SETTING

The Down Cliff Clay Member is a succession of claystones and siltstones up to 130 m thick that forms the lower part of the Bridport Sand Formation in the intra-cratonic Wessex Basin (Figs. 2A, 3; Buckman 1922; Howarth 1957; Cox et al. 1999; Morris et al. 2006; Hampson et al. 2015). The upper part of the Bridport Sand Formation is a gradationally based, intensely bioturbated, storm-dominated shoreface-shelf sandstone unit (Davies 1969; Bryant et al. 1988; Morris et al. 2006). In combination, the Down Cliff Clay Member and Bridport Sand Formation form an upward-coarsening, net-regressive interval of Toarcian (lower Jurassic) age that is overlain by the net-transgressive limestones of the Inferior Oolite Group (Fig. 3; Hesselbo and Jenkyns 1998). The Down Cliff Clay Member overlies the Beacon Limestone Formation (Fig. 3), formerly referred to as the Junction Bed (e.g. Buckman 1922), which is locally subdivided into the Marlstone Rock Member and overlying Eype Mouth Limestone Member (Cox et al. 1999). The Beacon Limestone is interpreted as net-transgressive (Hesselbo and Jenkyns 1998). Ammonite faunas in the Jurassic strata of the Wessex Basin define biostratigraphic zones and subzones (Fig. 3A). Basin-wide diachroneity in deposition of the Bridport Sand Formation and Down Cliff Clay Member is resolved in the framework of these ammonite zones and subzones (Buckman, 1889) (Fig. 3B).

During the early Jurassic, the Wessex Basin and adjacent areas underwent rifting across a series of west-east-trending extensional faults that bounded graben and half-graben depocentres, as well as regional subsidence (e.g. Jenkyns and Senior 1991; Hawkes et al. 1998). The thickness of the stratigraphic interval combining the Beacon Limestone Formation, Down Cliff Clay Member, Bridport Sand Formation, and Inferior Oolite Group is controlled by these fault-bounded depocentres, and reaches up to 270 m (Hawkes et al. 1998; Morris et al. 2006). In a regional context, the Wessex Basin and surrounding areas were occupied by a shallow seaway flanked by low-relief landmasses (inset map in Fig. 2A) at a paleolatitude of 30-40° N (e.g. Röhl et al. 2001).

The Bridport Sand Formation and Down Cliff Clay Member both contain seismically resolved southward-dipping clinoforms that indicate overall progradation from north to south (Hampson et al. 2015), consistent with biostratigraphic data that indicate southward-younging of the Bridport Sand Formation (Buckman 1889). However, eastward-dipping clinoforms that indicate local progradation from west to east are noted in the Wytch Farm oil field (Henk and Ward 2001; Morris et al. 2006) and at some outcrops (Ham Hill Quarry; fig. 16 in Morris et al. 2006). Bioclastic limestone units at specific levels in the Bridport Sand Formation mark transgressions and associated hiatuses in clastic sediment input (Knox et al. 1982; Morris et al. 2006), and bound clinoform sets in the Bridport Sand Formation (e.g. fig. 16 in Morris et al. 2006). Using the model of compound clinoforms outlined above (Fig. 1), Hampson et al. (2015) interpreted four subaqueous clinoform sets in the Down Cliff Clay Member using regional 2D seismic data, with set boundaries (shown in green in Fig. 2) marked by discordances in the apparent strike and progradation direction of clinoforms within sets (shown in orange in Fig. 2B), and coeval series of subaerial clinoform sets in the Bridport Sand Formation, with set boundaries marked by bioclastic limestone units. The petrography of the Bridport Sand Formation indicates that sediment was supplied from a southwestward-lying landmass in northwestern France (Boswell 1924; Davies 1969; Morton 1982), implying the existence of a tortuous sediment routing system from this landmass into the northwestern part of the Wessex Basin. Regional well data indicate that the Bridport Sand Formation pinches out to the east (Fig. 2A; Ainsworth et al. 1998; Hawkes et al. 1998).

DATA AND METHODS

This study builds on the previous work on the Bridport Sand Formation of Morris et al. (2006) and Hampson et al. (2015), who used a database of wireline log data from 126 wells distributed throughout the Wessex Basin, 400 km of 2D regional seismic lines, 150 km^2 of 3D seismic data from the Wytch Farm Field, 650 m of core from 12 wells, and measured sections from inland and coastal outcrops (Figs. 2A, 4A). The outcrop and core data analysed by Morris et al. (2006) and Hampson et al. (2015) and corresponding data used in previous sedimentologic studies (Davies 1967, 1969; Hounslow 1987; Bryant et al. 1988; Pickering 1995) were collected from the upper, sandstone-rich part of the Bridport Sand Formation. In this paper, we focus on the Down Cliff Clay Member (i.e. the lower, sandstone-poor part of the Bridport Sand Formation) using a complete, continuously cored section from the Winterborne Kingston no. 1 well (Rhys et al. 1982), in the context of observations from 2D and 3D seismic data (Fig. 4A). The Winterborne Kingston no. 1 well is tied to the GC73-28 2D regional seismic line using checkshot data, which was acquired in 1973 and is publically available from the UK Onshore Geophysical Library (www.ukogl.org.uk). The 3D seismic dataset was produced in 1998 by merging older offshore and onshore surveys over the Wytch Farm Field, and the data have been depth migrated and tied to wells through the generation of synthetic wavelets from two wells. The Down Cliff Clay Member crops out in inaccessible and partly overgrown coastal exposures (Buckman 1922; Howarth 1957; Hesselbo & Jenkyns 1995; Fig. 4A), but inland outcrops are not exposed.

Facies within the Down Cliff Clay Member were defined using a combination of conventional facies analysis and ichnofabric analysis of the core section. Facies analysis is based on observations of lithology, grain size and sorting, sedimentary structures, body fossils, and ichnofabrics. Ichnofabrics are modified from those documented by Morris et al. (2006) in the Bridport Sand Formation, and are defined using: (1) the intensity of bioturbation, as defined by the bioturbation index (BI) of Taylor and Goldring (1993); (2) the type, diversity and relative abundance of individual trace fossils; (3) cross-cutting relationships between trace fossils; (4) sand, silt, and clay content; and (5) physical sedimentary structures, where preserved. Biostratigraphic data for, and zonation of, the Down Cliff Clay Member in the Winterborne Kingston no. 1 well have been documented by Ivimey-Cook (1982).

COMPOUND CLINOFORMS IN THE BRIDPORT SAND FORMATION

Clinoforms imaged in 3D seismic data, Wytch Farm oil field

3D seismic data from the Wytch Farm oil field indicate that the Bridport Sand Formation and Down Cliff Clay Member contain clinoforms that dip at 2-3° towards the east and north-east (Henk and Ward 2001; Morris et al. 2006; Hampson et al. 2015) (Fig. 4B-E). In plan view, the clinoforms are gently curvilinear along depositional strike (Fig. 4B-C). Two distinct, vertically stacked clinoform sets are present in the Wytch Farm Field: the upper clinoform set occurs in the Bridport Sand Formation, and the lower clinoform set occurs in the Down Cliff Clay Member and downlaps on to the Beacon Limestone Formation (Fig. 4D-E). The contact between the two clinoform sets was originally interpreted as a flooding surface marked by downlap and an abrupt increase in water depth (e.g. Morris et al. 2006). More recently, some clinoforms in the two sets have been interpreted to be contiguous, such that they describe a "compound clinoform" geometry (e.g. "clinoform 2" in 4D-E) (Hampson et al., 2015). In this interpretation, the upper steeply dipping part of a compound clinoform defines a "subaerial clinoform" that comprises shoreface sandstones of the Bridport Sand Formation (cf. Fig. 6 of Morris et al. 2006), and the lower steeply dipping part of a compound clinoform defines a "subaqueous clinoform" in the Down Cliff Clay Member. The near-horizontal platform that separates these two steeply dipping parts of the compound clinoform is marked locally by toplap, offlap and downlap (e.g. "clinoforms 3-7" in 4D-E).

Clinoforms imaged in regional 2D seismic data, Wessex Basin

Regional 2D seismic data from parts of the Wessex Basin adjacent to the Wytch Farm field (Fig. 4A) also show distinct clinoform sets in the Down Cliff Clay Member and the Bridport Sand Formation. Clinoforms appear to dip at 1-5°, although their morphology is less clearly imaged than in 3D seismic data from the Wytch Farm oil field (e.g. Fig. 5; Fig. 4B-F of Hampson et al. 2015). At any particular location, the Down Cliff Clay Member contains a single clinoform set that downlaps on to the Beacon Limestone Formation (or an associated reflector). However, several laterally offset clinoform sets of different age have been interpreted over the Wessex Basin as a whole ("subaqueous clinoform sets 1-4" in Fig. 2A), recording the punctuated progradation of the Down Cliff Clay Member towards the south (Hampson et al. 2015). Clinoform set boundaries within the Down Cliff Clay Member (shown in green in Fig. 2) are marked by discordances in the strike orientation and local progradation direction of clinoforms within sets (shown in orange in Fig. 2B; Hampson et al., 2015). Clinoforms within the Bridport Sand Formation are thinner, and at any particular location occur either as a single set or multiple sets that exhibit some degree of vertical stacking (e.g. Fig. 5). Clinoform set boundaries are interpreted to be marked by bioclastic limestones, which formed during periods of condensed clastic sedimentation (Morris et al. 2006; Hampson et al. 2015).

In the vicinity of the Winterborne Kingston no. 1 well, clinoform geometries imaged in the Down Cliff Clay Member in 2D seismic data (Fig. 5) are corroborated by high-resolution dipmeter measurements, which indicate a consistent 2° dip towards the southeast in much of the unit (1026-1088 m; Knox et al. 1982; Rhys et al. 1982). Dipmeter measurements in the overlying Bridport Sands and underlying Middle Lias siltstones and sandstones record highly variable dips and azimuths, probably as a result of intense bioturbation and carbonate-cemented nodules obscuring primary bedding.

FACIES ANALYSIS AND FACIES SUCCESSION

Eight facies have been distinguished in the cored section. The characteristics of these facies are summarised in Table 1. Facies are grouped into four facies associations that are described below. The facies succession in the Winterborne Kingston core is summarised in Figure 6.

Facies Association A: downlapped substrate

Description.--- Facies association A is composed of beds of bioclastic sandy limestones (facies 1; Table 1) intercalated with thin (0.1 m) intervals of fossiliferous claystones and siltstones (facies 2; Table 1). Sandy limestones consist of upward-fining beds that are 0.1-0.4 m thick, some of which have coarse-grained lags, and which are stacked into units 0.5-2.5 m thick (Fig. 6). Bed bases are erosional, and many are associated with unlined, passively filled *Thalassinoides* burrows. Bioclasts are transported and commonly fragmented, and include ammonites, belemnites, crinoids, brachiopods, and bivalves (Figs. 6, 7A-B). Fine sand grains are also abundant in the lower part of the succession, and are similar in grain size and texture to sand in the directly underlying Middle Lias Silts and Sands succession (Fig. 6). Bioclastic sandy limestones (facies 1) are sparsely to completely bioturbated (BI: 1-6) by *Terebellina*, *Thalassinoides*, *Planolites*, *Palaeophycus*, and small *Arenicolites* (Fig. 7A-B). Thin (0.1-0.2 m) intervals of moderately to highly bioturbated (BI: 3-4, by *Chondrites*), fossiliferous claystones and siltstones (facies 2) are intercalated between limestone units (Fig. 7C). Lithological contacts between the bioclastic sandy limestones (facies 1) and fossiliferous claystones and siltstones (facies 2) are commonly nodular or diffuse in character (Fig. 7A-B), and are marked by pronounced differential compaction of the claystones and siltstones.

Interpretation.--- The abundance of transported and fragmented bioclasts in facies association A implies energetic physical reworking under conditions of low siliciclastic sediment supply. The body fossil assemblage constitutes a fully marine nektos (ammonites, belemnites) and benthos (crinoids, bivalves, brachiopods) (Ivimey-Cook 1982). Fine sand grains in the lower part of facies association A were probably reworked from the underlying Middle Lias Silts and Sands succession, consistent with the erosional base of the facies association. Erosionally based, upward-fining, sandy limestone beds are interpreted to record episodic depositional events, and the unlined, passively filled *Thalassinoides* burrows at bed bases are interpreted to constitute Glossifungites ichnofacies developed in erosionally exhumed, firmground substrates (MacEachern et al. 1992). Bioturbation in these sandy limestone beds records biogenic sediment reworking in between depositional events. The high diversity trace fossil assemblage in these beds (facies 1) constitutes a mixture of Cruziana and Skolithos ichnofacies (MacEachern & Bann 2008), indicating shallow, fully marine conditions. Fossiliferous claystone and siltstone intervals (facies 2) record deposition of clay under more quiescent conditions. Nodular and diffuse bed boundaries between bioclastic sandy limestones (facies 1) and fossiliferous claystones and siltstones (facies 2) result from early calcite cementation, as indicated by differential compaction across the boundaries.

Overall, the succession represented by facies association A is characterised by upward-fining in grain size, increasing-upward preservation of depositional event beds and intervening claystones and siltstones, and an upward decrease in the proportion of benthic body fossils (brachiopods, bivalves) relative to nektonic body fossils (ammonites, belemnites) (Fig. 6). These characteristics indicate that the succession is net-transgressive and records an upward increase in water depth.

Facies Association B: subaqueous clinoform foreset-to-toeset transition

Description.--- Facies association B consists predominantly of non- to highly bioturbated claystones and siltstones (facies 3; Table 1) that contain nodular, calcareous claystones and siltstones (facies 4; Table 1) (Fig. 7D-F). Nodular, calcareous claystones and siltstones decrease in abundance from base to top of the association (Fig. 6). The lowermost part of the facies association comprises a thin (0.2 m) interval of fossiliferous claystones and siltstones (facies 2; Table 1), and the upper part of the association contains rare, thin (0.1 m) intervals of moderately to completely bioturbated siltstones (facies 5; Table 1) (Fig. 6). The intensity of bioturbation varies from absent to high (BI: 0-4), and is characterised by *Chondrites* with less abundant *Planolites* and *Thalassinoides* in much of the facies association (facies 2, 3, 4) (Fig. 7D-F). Claystones and siltstones contain parallel lamination where physical structures are not obscured by bioturbation (Fig. 7E), and calcite-cemented nodules are associated with differential compaction of surrounding claystones and siltstones (Fig. 7D-E). Body fossils are sparse, but include ammonites, belemnites, brachiopods, bivalves, and fragmented bioclasts (Figs. 6, 7D-E). Moderately to completely bioturbated siltstones (facies 5) are more intensely bioturbated (BI: 3-6) by *Terebellina* (*sensu lato*), *Helminthopsis*, small *Teichichnus*, *Chondrites*, *Planolites*, and *Anconichnus*, and contain only rare belemnites.

Facies association B corresponds to the toesets of the Down Cliff Clay clinoforms (Fig. 5), which downlap onto the underlying Beacon Limestone Formation (or an associated reflector). The facies association is associated with variable dips and azimuths in the high-resolution dipmeter log, reflecting the irregular boundaries of carbonate-cemented nodules (Knox et al. 1982; Rhys et al. 1982).

Interpretation.--- The fine-grained, predominantly siliciclastic character of facies association B implies a high supply of clay and silt relative to facies association A. Primary sedimentary structures are only sparsely preserved, due to overprinting by bioturbation and nodular calcite cementation, but parallel lamination is attributed to deposition from suspension fall-out and from distal sediment gravity flows (cf. Bouma d-e sequences in turbidite beds, or b-c units in wave-enhanced sediment gravity flow beds; Macquaker et al. 2010). Bioturbation is generally low in diversity (facies 3, 4; Table 1), and locally monospecific (facies 2; Table 1), implying persistent physico-chemical stress during deposition (e.g. MacEachern and Bann 2008; Gingras et al. 2011). Body fossil assemblages indicate a consistently fully marine nektos (ammonites, belemnites) and benthos (bivalves, brachiopods) (Ivimey-Cook 1982), although the latter may have been transported from shallower water depths, which implies that chemical stress arose from intermittent and/or poor oxygenation of bottom waters. Similar low-diversity trace fossil assemblages dominated by *Chondrites* are common in successions deposited under largely dysoxic conditions (e.g. Bromley and Ekdale 1984; Savrda and Bottjer 1989; MacQuaker and Gawthorpe 1993; Ghadeer and MacQuaker 2011). Bed-scale variations in bioturbation intensity may reflect variable sedimentation rate (e.g. MacQuaker and Howell 1999; Ghadeer and MacQuaker 2011; Gingras et al. 2011). This interpretation is supported by similar bed-scale variations in bioclast abundance and associated early-diagenetic calcite cement, which also probably result from variable suspension fall-out and/or (bioclastic) sediment transport rates. Bioturbation diversity and intensity increase in the upper part of the succession (facies 5, containing the Helminthopsis and Anchonichnus motting ichnofabrics of Morris et al. 2006; Table 1), indicating more consistent oxygenation of bottom waters.

Facies Association C: subaqueous clinoform foreset

Description.--- Facies association C comprises moderately to completely bioturbated siltstones (facies 5; Table 1) and moderately to intensely bioturbated, sandy siltstones (facies 6; Table 1). Bioturbation intensity varies from moderate to complete (BI: 3-6), and is characterised by *Terebellina* (sensu lato), *Helminthopsis*, *Zoophycos*, *Asterosoma*, small *Teichichnus*, *Chondrites*, *Planolites*, and *Anconichnus* (Fig. 7G-I). Subtle variations in grain size and bioturbation intensity define remnant centimetre-scale bedding. Where preserved, physical structures include erosional scours at the base of thin (<1 cm) siltstone and very fine-grained sandstone beds, parallel lamination, and rare current-ripple cross-lamination (Figs. 6, 7J-N). The tops of some beds contain mottling by *Anconichnus* traces (Fig. 7J). Rare belemnites are the only body fossils present.

Facies association C corresponds to the foresets of the Down Cliff Clay clinoforms (Fig. 5), and contains consistent dips of 2° towards the southeast in the high-resolution dipmeter log (Knox et al. 1982; Rhys et al. 1982).

Interpretation.--- The siltstone-dominated character of facies association C, abundance of centimetre-scale remnant bedding, and paucity of body fossils imply rapid sedimentation and a high supply of silt, relative to underlying facies association B. Thin siltstone and very fine-grained sandstone beds record episodic influxes of silt and sand. The erosional bases of these beds and the occurrence of parallel lamination and current-ripple cross-lamination within them indicate that they record erosion and subsequent deposition by waning, unidirectional tractional currents. The waning-flow beds are interpreted as distal turbidites (cf. Bouma b-e and c-e sequences) and/or wave-enhanced sediment gravity flow beds (a-c units of Macquaker et al. 2010). These event beds may have been triggered by storm waves and/or river floods, as noted in similar successions (e.g. Bentley and Nittrouer 2003; Ghadeer and MacQuaker 2011; Plint 2014); however, the former appears the more likely mechanism, given the storm-dominated character of deposition in the overlying shoreface sandstones of the Bridport Sand Formation (Morris et al. 2006). The high diversity of trace fossil assemblages in the facies association implies deposition in well-oxygenated, fully marine bottom waters that lacked significant physico-chemical stress (e.g. MacEachern and Bann 2008; Gingras et al. 2011), most likely reflecting “background” sedimentation between event-bed deposition (i.e. Helminthopsis and Terebellina 1 ichnofabrics of Morris et al. 2006). This interpretation is consistent with deposition above effective storm wave base, above which the water column was mixed by storms, but below fairweather wave base. *Anconichnus* traces at the tops of some event beds are interpreted to reflect opportunistic colonization of the sea bed after storm events (i.e. Anchonichnus motting ichnofabric of Morris et al. 2006).

Facies Association D: subaqueous clinoform topset

Description.--- Facies association D consists of a thin (0.7 m) interval of iron-stained, oolitic siltstones (facies 7; Table 1) and chloritic siltstones (facies 8; Table 1), which occurs within moderately to completely bioturbated siltstones (facies 5; Table 1) and moderately to intensely bioturbated, sandy siltstones (facies 6; Table 1) of facies association C. Red, iron-stained and phosphatic ooids, phosphate pebbles, and fragmented and abraded body fossils are common and characteristic of facies association D. These clasts occur within a siltstone and sandy siltstone matrix (Fig. 7O-P). Body fossils include ammonites, belemnites, bivalves, and gastropods (Figs. 6, 7O-P). Siltstones are either red or green in colour (in facies 7 and 8, respectively), the latter due to a high chlorite content (Knox 1982). Bioturbation varies from low intensity (BI: 2) by monospecific *Chondrites*, to high intensity (BI: 4) by *Terebellina* (sensu lato), *Helminthopsis*, *Zoophycos*, *Asterosoma*, small *Teichichnus*, *Chondrites*, and *Planolites*.

Facies association D occurs in the topsets of the Down Cliff Clay clinoforms (Fig. 5). The facies association lacks consistent dips and azimuths in the high-resolution dipmeter log (Knox et al. 1982; Rhys et al. 1982).

Interpretation.--- Iron-stained and phosphatic ooids, phosphate pebbles, and abraded body fossils in facies association D all indicate extended physical reworking of these grains. The shape and internal structure of the phosphatic ooids implies that they were originally composed of chamosite (Knox et al. 1982), while the high chlorite content of associated siltstones is interpreted as the product of alteration from chamosite (Knox 1982; Knox et al. 1982). Chamosite precipitation would have required a relatively high supply of iron via input of terrigenous clays into a warm shallow-marine environment, together with siliciclastic sediment starvation to allow iron enrichment (Young 1989). Extended physical reworking of chamosite ooids and other grains was most likely due to waves, given the abundance of wave-generated structures in the overlying Bridport Sands Formation (Morris et al. 2006), but the occurrence of these grains in a siltstone matrix suggests that they were reworked and transported. The facies association is therefore interpreted to represent condensed sedimentation under energetic conditions. Variation in the diversity of bioturbation implies a variable physico-chemical stress (e.g. MacEachern and Bann 2008; Gingras et al. 2011), possibly due to temporal changes in oxygenation of bottom waters.

Facies succession and sequence stratigraphy

Description.--- The lower part of the studied facies succession comprises limestone-rich deposits of facies association A overlain by an interval of facies association B that is rich in nodular, calcareous claystones and siltstones (facies 4) (1102-1118 m in Fig. 6). This part of succession also contains abundant biozones (e.g. labelled "T1" to "T5" in the lower Down Cliff Clay Member; 1102-1115 m in Fig. 6).

The upper part of the facies succession comprises a carbonate-poor interval of facies association B that passes gradationally upwards into facies association C and is then truncated by facies association D (1016-1102 m in Fig. 6). This part of the succession comprises the upper Down Cliff Clay Member and overlying deposits of the Bridport Sand Formation, and contains few biozones (labelled "T6" to "T9"; Fig. 6). The thin (0.2-0.3 m) interval of facies association D that caps the studied facies succession contains one biozone ("T10"; Fig. 6).

Interpretation.--- The lower part of the studied facies succession records an overall upward increase in water depth, from an agitated, well-oxygenated sea floor that lay above fairweather wave base (facies 1) to an intermittently and/or poorly oxygenated sea floor that lay at or below effective storm wave base (facies 3, 4) (Table 1; Fig. 6). This lower part of the succession also contains an upward decrease in the proportion of benthic body fossils (brachiopods, bivalves) relative to nektonic body fossils (ammonites, belemnites) (Fig. 6). The lower 2 m of the succession is marked by erosion and reworking of sand grains from the underlying Middle Lias Silts and Sands (facies 1). In combination, these characteristics indicate that the lower part of the studied succession is net transgressive, as interpreted by Hesselbo and Jenkyns (1998), with a transgressive erosion surface at its base and a maximum flooding surface at its top. The maximum flooding surface is interpreted to be downlapped by seismically imaged clinoforms in the Down Cliff Clay Member (Fig. 5).

The upper part of the facies succession records upward shallowing from an intermittent and/or poorly oxygenated sea floor below effective storm wave base (facies 3, 4) to a sea floor that aggraded via intermittent deposition from sediment gravity flows and tractional currents above effective storm wave base (facies 5, 6) (Table 1; Fig. 6). This interval is interpreted to correspond to seismically imaged clinoforms in the Down Cliff Clay Member (Fig. 5), consistent with the 2° dip towards the southeast noted in high-resolution dipmeter measurements (1026-1088 m in Fig. 6; Knox et al. 1982; Rhys et al. 1982). The succession is regressive, as interpreted by Hesselbo and Jenkyns (1998), and is truncated by erosionally based, winnowed lag deposits that record extended physical reworking (facies 7, 8) (Table 1; 1016 m in Fig. 6). Previously, such lag deposits have been interpreted as transgressively reworked sequence boundaries (Morris et al. 2006; their figure 13), but this interpretation is contradicted by the absence of a facies dislocation across the lag (i.e. intercalated successions of facies 5 and 6 lie above and below the lag; Fig. 6). In the context of the "compound clinoform" interpretation of the Bridport Sand Formation proposed by Hampson et al. (2015; their figure 5A), the lag represents the near-horizontal subaqueous platform that separates the "subaerial clinoform" of the Bridport Sand shoreface sandstones from the "subaqueous clinoform" of the Down Cliff Clay Member. The winnowed character of the lag is consistent with sediment bypass across this near-horizontal subaqueous platform (cf. Swenson et al. 2005; Mitchell 2012).

DISCUSSION

Sediment transport along Down Cliff Clay Member clinoforms

The facies interpretations presented above are synthesised into a model of the Down Cliff Clay Member subaqueous clinoforms (Fig. 8). Components of this model are described below.

Facies association B represents the toeset and lower foreset of the subaqueous clinoform, as indicated by high-resolution dipmeter data (1086-1102 m in Fig. 6), where deposition occurred principally from suspension fallout of clay and silt below effective storm wave base (facies 3, 4). The sea floor was intermittently and/or poorly oxygenated, perhaps reflecting only rare mixing of the deep part of the water column by storms. Subaqueous clinoform toeset and lower foreset deposits record 16 m of vertical sediment accumulation in 3.3 Myr, based on biozone occurrence ("T5" to "T8" in Fig. 6) calibrated to the age model of Ogg and Hinnov (2012) (Fig. 3A), giving a mean sediment accumulation rate of 4.4 m/Myr. This rate does not account for decompaction.

Facies association C represents the steeply paleoseaward-dipping (2° eastward-dipping; Figs. 5, 6) subaqueous clinoform foreset (1016-1086 m in Fig. 6), where deposition of silt and very fine sand occurred from intermittent sediment gravity flows and tractional currents above effective storm wave base (facies 5, 6). The overlying Bridport Sands Formation contains abundant evidence for storm wave action (Morris et al. 2006), implying that storms were the most likely trigger for the sediment gravity flows and tractional currents, although river floods and strong, episodic tidal currents and geostrophic oceanographic currents cannot be discounted. Additional silt was supplied by suspension fallout. The near-linear planform geometry of the subaqueous clinoforms (Fig. 4B-C) implies a strong component of shore-parallel sediment transport (cf. Cattaneo et al. 2003). In the northerly paleolatitudes of the Wessex Basin (30-40° N; e.g. Röhl et al. 2001), cyclonic circulation during storms would have been counter-clockwise, due to deflection by Coriolis force, thus providing a mechanism for southwestward-directed, shore-parallel sediment transport on Down Cliff Clay clinoform foresets developed along the western margin of the Wessex Basin. Subaqueous clinoform foreset deposits record 70 m of vertical sediment accumulation in 0.4 Myr, based on biozone occurrence ("T8" to "T10" in Fig. 6) calibrated to the age model of Ogg and Hinnov (2012) (Fig. 3A), giving a mean, undecompacted sediment accumulation rate of 194 m/Myr (Fig. 9C).

Facies association D records sediment bypass and winnowing of the subaqueous clinoform topset, as indicated by iron-stained and phosphatic ooids, phosphatic pebbles, and fragmented and abraded body fossils (facies 7, 8). Winnowing of the topset is interpreted to record high bed shear stresses, which exceeded the local threshold of motion for very fine sand, during major storms (e.g. Mitchell et al. 2012). High bed shear stresses were also potentially augmented by tides. In this interpretation, the near-horizontal subaqueous platform that forms the winnowed topset of the Down Cliff Clay clinoforms approximates the inner, sandy part of a wave-graded shelf (Johnson 1919). The shoreface sandstones of the Bridport Sand are interpreted to form the subaerial clinoform (cf. Morris et al. 2006). The shoreface is interpreted to have been supplied by fluvial sediment influx that was dispersed by longshore currents, which were generated by the oblique approach of fairweather waves and/or by tidal currents. Subaqueous clinoform topset deposits record <1 m of vertical sediment accumulation in a single biozone ("T10" in Fig. 3B), such that a mean sediment accumulation rate cannot be calculated. However, the three overlying, vertically stacked subaerial clinoform sets in combination with the subaqueous clinoform topset deposits record 88 m of vertical sediment accumulation in <0.2 Myr, based on biozone occurrence ("T10" to "T11" in Fig. 3B) calibrated to the age model of Ogg and Hinnov (2012) (Fig. 3A), giving a mean, undecompacted sediment accumulation rate of 489 m/Myr.

Comparison with modern subaqueous-deltaic clinoforms

The processes interpreted in the Down Cliff Clay Member subaqueous clinoforms (Fig. 8) are similar to those documented or inferred in modern subaqueous-deltaic clinoforms. In both modern deltas and the Down Cliff Clay Member, deposition on the subaqueous clinoform foreset is largely via intermittent sediment gravity flows and/or tractional currents that result from sediment bypass due to waves, tides or other oceanographic currents that sweep across the clinoform topset (Fig. 8). The palaeogeographic context of the Down Cliff Clay Member is unclear, and a major fluvial source(s) of sediment to the coeval shoreline has not been identified. Instead, the Bridport Sand Member represents a wave-dominated shoreface with localised, subordinate tidal influence (Davies 1969; Hounslow 1987; Morris et al. 2006). As a result, we infer that fluvial sediment influx to the Bridport Sand Member and Down Cliff Clay Member was probably via a number of minor rivers, such as the Apennine rivers that act as a "line source" for the western Adriatic subaqueous clinoform (Cattaneo et al. 2003, 2007).

The geometry of the Down Cliff Clay Member subaqueous clinoforms differs from those of well-documented, modern subaqueous-deltaic clinoforms (e.g. Ganges-Brahmaputra Delta, Michels et al. 1998; Po Delta and western Adriatic shelf, Cattaneo et al. 2003, 2007; Yellow River Delta, Liu et al. 2004; Yangtze River Delta, Liu et al. 2006). The modern subaqueous-deltaic clinoforms have a comparable height (30-70 m) to the Down Cliff Clay Member subaqueous clinoforms (c. 80 m compacted thickness, and c. 100 m decompacted thickness using the shaly sand curve of Sclater and Christie 1980). However, the Down Cliff Clay Member subaqueous clinoforms dip at 2-3° after compaction (2-4° if decompacted), whereas modern subaqueous-deltaic clinoforms dip at 0.1-0.5° prior to compaction (Michels et al. 1998; Cattaneo et al. 2003, 2004, 2007; Liu et al. 2004, 2006; Fig. 9). The latter generally occur as part of continent-scale sediment routing systems associated with some of the world's major rivers, with correspondingly large sediment discharges (Milliman and Meade 1983). The size of the Bridport Sand Formation and Down Cliff Clay Member sediment routing system is less clear, although provenance analysis implies a sediment source from a low-relief landmass in northwestern France (Boswell 1924; Davies 1969; Morton 1982) and a relatively small, tortuous sediment routing system. The steep dips of the Down Cliff Clay Member subaqueous clinoforms may reflect a lower rate of sediment supply than for the modern subaqueous-deltaic clinoforms. However, they may also reflect the prevalence of early-diagenetic carbonate cementation, in the form of concretionary horizons, which stabilised the Down Cliff Clay Member subaqueous clinoforms, and thus allowed steep clinoform foresets to be constructed and maintained.

Sediment accumulation rates are also very different on the foresets of the Down Cliff Clay Member subaqueous clinoforms (0.02 cm/yr measured over 100 kyr time scale) and modern subaqueous-deltaic clinoforms (0.6-6.8 cm/yr measured over 0.1 kyr time scale, and 0.08-0.2 cm/yr measured over 1 kyr time scale; Michels et al. 1998; Cattaneo et al. 2003, 2004, 2007; Vigliotti et al. 2008) (Fig. 9). Compaction plays only a minor role in this discrepancy. Instead, the 1-2 order-of-magnitude difference in sediment accumulation rates can largely be attributed to the 2-3 order-of-magnitude difference in timescales over which they have been measured (Sadler 1981), although differences in sediment supply between the Bridport Sand Formation and Down Cliff Clay Member sediment routing system and its modern counterparts cannot be ruled out. Cattaneo et al. (2003) and Vigliotti et al. (2008) noted pronounced variability in the Holocene western Adriatic shelf subaqueous clinoform set, with condensed deposition alternating with increments of enhanced progradation, such as that for which recent sediment accumulation rates have been measured. Such variations in short-term in sediment accumulation rate are averaged to give a much slower long-term sediment accumulation rate.

Clinoform progradation rate

Using the estimated mean sediment accumulation rate of 194 m/Myr (after compaction) and dip angle of 2° for the foreset of the Down Cliff Clay Member subaqueous clinoforms, and assuming a horizontal clinoform trajectory in the direction of clinoform-foreset dip (cf. shoreline trajectory) that is consistent with the very slow vertical accumulation of the clinoform topsets and toesets, the long-term progradation rate of the clinoforms intersected by the Winterborne Kingston no. 1 well was c. 5.6 km/Myr (c. 6.7 km/Myr accounting for decompaction). Based on regional mapping constrained by ammonite biozones, which were calibrated to the age model of Ogg and Hinnov (2012), Hampson et al. (2015) estimated that each subaqueous clinoform set had a c. 0.5 Myr duration and represents 6-42 km of progradation (e.g. Fig. 2). Shorter progradation distances occur in fault-bounded grabens, such as the Winterborne Trough that contains the Winterborne Kingston no. 1 well (cf. the extent of “subaqueous clinoform set 3” in Fig. 2A; Hampson et al. 2015). These grabens contain thickened successions of lower Jurassic strata and underwent relatively rapid subsidence (Hawkes et al. 1998). The estimated durations, progradation distances and long-term progradation rates given above are consistent, at least as first-order approximations. It is also clear that subaerial clinoforms migrated more quickly than subaqueous clinoforms, because they are associated with a faster mean sediment accumulation rate (e.g. 489 m/Myr in the Winterborne Kingston no. 1 well, after compaction), and multiple, vertically stacked subaerial clinoform sets are developed coeval with a single subaqueous clinoform set (Hampson et al. 2015; see also “subaqueous clinoform set 4” and “subaerial clinoform sets 4” in Fig. 3B). Thus, the shoreline, as represented by subaerial clinoforms, was more mobile and underwent more frequent regressive-transgressive transits than the subaqueous clinoforms.

Implications for recognition of ancient muddy subaqueous-deltaic clinoforms

The relative scarcity of muddy subaqueous-deltaic clinoforms interpreted in the stratigraphic record, compared to the abundance of their modern counterparts, implies that they are under-recognised. The Down Cliff Clay Member meets the five diagnostic criteria suggested by Cattaneo et al. (2003) for ancient subaqueous-deltaic clinoforms, based on the Holocene western Adriatic shelf subaqueous clinoform set, because it contains: (1) low-angle clinoform foresets (Figs. 4D-E, 5); (2) offlap breaks at the clinoform topset-to-foreset transition that lie seaward of the coeval shoreline; (3) laterally extensive, linear-to-gently-curved clinoforms in plan view (Figs. 2B, 4B-C); (4) fully marine facies and fauna in the clinoform topsets (1015-1017 m in Fig. 6; Fig. 7O-P); and (5) has relatively uniform grain size (Fig. 6). Clinoform foresets in the Down Cliff Clay Member are much steeper than their modern counterparts (Fig. 9), such that they can be imaged in dipmeter logs (Knox et al. 1982; Rhys et al. 1982) as well as in seismic data, and they are probably unusual in this regard (Patruno et al. 2015b).

Continuous core through the Down Cliff Clay Member allows these diagnostic criteria to be refined by the addition of more detailed sedimentologic characteristics. Subaqueous-deltaic clinoform foresets have rapid sedimentation rates, relative to overlying and underlying mud-prone successions that represent clinoform topsets and bottomsets, respectively. Variations in sedimentation rate between clinoform topsets, foresets and bottomsets are recorded by high-resolution biostratigraphic data, where available, and by bed-scale sedimentologic observations in outcrop and core. Clinoform-topset deposits contain winnowed bypass surfaces and lags. Clinoform foresets accumulated by deposition from episodic waning tractional currents, such as distal turbidites and wave-enhanced sediment gravity flows. Clinoform toeset deposits record mainly condensed pelagic sedimentation.

CONCLUSIONS

The Lower Jurassic Down Cliff Clay Member of the Bridport Sand Formation, Wessex Basin, UK contains seismically imaged examples of muddy subaqueous-deltaic clinoforms, which are a common feature of modern deltas but are only rarely documented in ancient strata. The Down Cliff Clay subaqueous-deltaic clinoforms are contiguous with, and occur beyond the palaeoseaward limit of, coeval subaerial(?) deltaic clinoforms in the stratigraphically higher, shoreface sandstones of the Bridport Sand Formation. In combination, the clinoforms in the Down Cliff Clay Member and Bridport Sand Formation define a compound clinoform morphology.

Facies analysis of continuous core data through the Down Cliff Clay subaqueous-deltaic clinoforms and related strata indicates that they consist of four facies associations, A-D, from base to top of the succession:

- Facies association A consists of erosionally based, bioclastic sandy limestone beds intercalated with upward-thickening fossiliferous claystones and siltstones, and contains trace fossil assemblages that constitute a mixture of Cruziana and Skolithos ichnofacies. The facies association records an upward increase in water depth under conditions of minor clastic sediment input and reworking by storm waves. These deposits are downlapped by the subaqueous-deltaic clinoforms.

- Facies association B comprises non- to highly bioturbated, variably laminated claystones and siltstones that contain calcareous nodules, and is characterised by low-diversity trace fossil assemblages dominated by *Chondrites*. The facies association records slow, episodic deposition from suspension fall-out and distal sediment gravity flows under conditions of intermittent and/or poor oxygenation of bottom waters. These deposits represent the foreset-to-toeset transition of the subaqueous-deltaic clinoforms.
- Facies association C consists of moderately to completely bioturbated siltstones and moderately to intensely bioturbated, sandy siltstones, both of which contain a high-diversity trace fossil assemblage. Where preserved, thin (<1 cm), erosionally based siltstone and very fine-grained sandstone beds contain parallel lamination and rare current-ripple cross-lamination. The facies association records episodic deposition by sediment gravity flows and tractional currents (e.g. distal turbidites, wave-enhanced sediment gravity flows) above effective storm wave base in well-oxygenated, fully marine bottom waters. These deposits represent the foresets of the subaqueous-deltaic clinoforms, which dip paleoseaward at 2°.
- Facies association D consists of iron-stained, oolitic siltstones and chloritic siltstones that are characterised by iron-stained and phosphatic ooids, phosphatic pebbles, and fragmented and abraded body fossils. The facies association records extended physical reworking, winnowing and sediment bypass. These deposits represent the topset of the subaqueous-deltaic clinoforms, which formed at the paleo-water depth at which the local threshold of motion for very fine sand was exceeded by bed shear stresses during major storms.

High-resolution biostratigraphic data calibrated to a globally standard age model indicate that mean, undecompacted sediment accumulation rates on the toeset and foreset of the Down Cliff Clay subaqueous-deltaic clinoforms were c. 4.4 m/Myr and 194 m/Myr, respectively. These long-term rates are consistent with those measured at centennial timescales in modern subaqueous-deltaic clinoforms, and imply a long-term clinoform progradation rate of c. 5.6 km/Myr (c. 6.7 km/Myr accounting for decompaction).

The facies model developed herein for the Down Cliff Clay Member, together with interpreted sediment transport mechanisms and long-term depositional rates, can potentially be applied to other ancient shallow-marine mudstone successions. This application may aid identification of subaqueous-deltaic clinoforms and compound clinoform morphologies, which are common in modern deltas, in the stratigraphic record.

ACKNOWLEDGMENTS

The authors gratefully acknowledge funding and support of KP via a scholarship under the royal patronage of Princess Maha Chakri Sirindhorn of Thailand, and access to the Winterborne Kingston. We thank Nick Holgate, Chris Jackson, Howard Johnson, Jenny Morris, and Stefano Patruno for insightful discussions of the Bridport Sand Formation, Down Cliff Clay Member, and compound clinoforms. We are grateful for the constructive review and editorial comments of Antonio Cattaneo, Tobi Payenberg, and Leslie Melim.

REFERENCES

Ainsworth, N.R., Braham W., Gregory, J.F., Johnson, B., & King, C., 1998, The lithostratigraphy of the latest Triassic to earliest Cretaceous of the English Channel and its adjacent areas, *in* Underhill, J.R., ed., Development, evolution and petroleum geology of the Wessex Basin: Geological Society of London, Special Publication 133, p. 103-164.

Asquith, D.O., 1970, Depositional topography and major marine environments, Late Cretaceous, Wyoming: AAPG Bulletin, v. 54, p. 1184-1224.

Bentley, S.J. & Nittrouer, C.A., 2003, Emplacement, modification, and preservation of event strata on a flood-dominated continental shelf: Eel shelf, Northern California: Continental Shelf Research, v. 23, p. 1465-1493.

Boswell, P.G.H., 1924, The petrography of the sands of the Upper Lias and Lower Inferior Oolite in the west of England: Geological Magazine, v. 31, p. 246-264.

Bromley, R.G. & Ekdale, A.A., 1984, *Chondrites*: a trace fossil indicator of anoxia in sediments: Science, v. 224, p. 872-874.

Bryant, I.D., Kantorowicz, J.D. & Love, C.F., 1988, The origin and recognition of laterally continuous carbonate-cemented horizons in the Upper Lias Sands of southern England: Marine and Petroleum Geology, v. 5, p. 109-131.

Buckman, S.S., 1889, On Cotteswold, Midford and Yeovil sands, and the division between Lias and Oolite: Quarterly Journal of the Geological Society of London, v. 45, p. 440-474.

Buckman, S.S., 1922, Jurassic chronology: II - preliminary studies. Certain Jurassic strata near Eypesmouth (Dorset): the Junction Bed of Watton Cliff and associated rocks: Quarterly Journal of the Geological Society of London, v. 78, p. 378-436.

Callomon, J.H. & Cope, J.C., 1995, The Jurassic Geology of Dorset, *in* Taylor, P.D., ed., Field Geology of the British Jurassic: Geological Society of London, p. 51-103.

Cattaneo, A., Correggiari, A., Langone, L., & Trincardi, F., 2003, The late-Holocene Gargano subaqueous delta, Adriatic shelf: sediment pathways and supply fluctuations: Marine Geology, v. 193, p. 61–91.

Cattaneo, A., Trincardi, F., Langone, L., Asioli, A. & Puig, P., 2004, Clinoform generation on Mediterranean margins: Oceanography, v. 17, p. 104-117.

Cattaneo, A., Trincardi, F., Asioli, A., & Correggiari, A., 2007, The western Adriatic shelf clinoform: energy-limited bottomset: Continental Shelf Research, v. 27, p. 506–525.

Cox., B.M., Sumbler, M.G. & Ivimey-Cook, H.C., 1999, A formational framework for the Lower Jurassic of England and Wales (onshore area): British Geological Survey, Research Report RR/99/01.

Davies, D.K., 1967, Origin of friable sandstone-calcareous sandstone rhythms in the Upper Lias of England: Journal of Sedimentary Petrology, v. 37, p. 1179-1188.

Davies, D.K., 1969, Shelf sedimentation: an example from the Jurassic of Britain: Journal of Sedimentary Petrology, v. 39, p. 1344-1370.

Driscoll, N.W. & Karner, G.D., 1999, Three-dimensional quantitative modelling of clinoform development: Marine Geology, v. 154, p. 383–398.

Ghadeer, S.G. & Macquaker, J.H.S., 2011, Sediment transport processes in an ancient mud-dominated succession: a comparison of processes operating in marine offshore settings and anoxic basinal environments: Journal of the Geological Society of London, v. 168, p. 1121-1132.

Gingras, M.K., MacEachern, J.A., & Dashtgard, S.E., 2011, Process ichnology and the elucidation of physico-chemical stress: Sedimentary Geology, v. 237, p. 115-134.

Hampson, G.J., 2010, Sediment dispersal and quantitative stratigraphic architecture across an ancient shelf: Sedimentology, v. 57, p. 96-141.

Hampson, G.J., Morris, J.E., & Johnson, H.D., 2015, Synthesis of time-stratigraphic relationships and their impact on hydrocarbon reservoir distribution and performance, Bridport Sand Formation, Wessex Basin, UK, *in* Smith, D.G., Bailey, R.J., Burgess, P.M., & Fraser, A.J., eds., Time and strata: probing the gaps in our understanding: Geological Society of London, Special Publication 404, p. 199-222.

Hawkes, P.W., Fraser, A.J., & Einchcomb, C.C.G., 1998, The tectono-stratigraphic development and exploration history of the Weald and Wessex Basin, Southern England, UK, *in* Underhill, J.R., ed., Development, evolution and petroleum geology of the Wessex Basin: Geological Society of London, Special Publication 133, p. 39-65.

Henk, F.G. & Ward, G.S., 2001, The Bridport Sandstone of the Wytch Farm Oil Field, a shelf sandbody or shoreface?: an ichnological and 3-D seismic sequence stratigraphic investigation into the shallow marine origin (abstract): AAPG, Annual Convention Program 10, p. A84.

Hesselbo, S.P. & Jenkyns, H.C., 1995, A comparison of the Hettangian to Bajocian successions of Dorset and Yorkshire, *in* Taylor, P.D., ed., Field Geology of the British Jurassic: Geological Society of London, p. 105-150.

Hesselbo, S.P. & Jenkyns, H.C., 1998, British Lower Jurassic sequence stratigraphy, *in* de Graciansky, P-C., Hardenbol, J., Jacquin, T. & Vail, P.R., eds., Mesozoic and Cenozoic sequence stratigraphy of European basins: SEPM, Special Publication 60, p. 561-581.

Hounslow, M.W., 1987, Magnetic fabric characteristics of bioturbated wave-produced grain orientation in the Bridport-Yeovil Sands (Lower Jurassic) of Southern England: Sedimentology, v. 34, p. 117-128.

Howarth, M.K., 1957, The Middle Lias of the Dorset coast: Quarterly Journal of the Geological Society, v. 113, p. 185-204.

Ivimey-Cook, H.C., 1982, Biostratigraphy of the Lower Jurassic and Upper Triassic (Rhaetian) rocks of the Winterborne Kingston borehole, Dorset, *in* Rhys, G.H., Lott, G.K., & Calver, M.A., eds., The Winterborne Kingston borehole, Dorset: Report of the Institute of Geological Sciences 81/3, p. 97-106.

Jenkyns, H.C. & Senior, J.R., 1991, Geological evidence for intra-Jurassic faulting in the Wessex Basin and its margins: Journal of the Geological Society, v. 148, p. 245-260.

Johnson, D.W., 1919, Shore processes and shoreline development: John Wiley & Sons.

Knox, R.W.O.B., 1982, Clay mineral trends in cored Lower and Middle Jurassic sediments of the Winterborne Kingston borehole, Dorset, *in* Rhys, G.H., Lott, G.K., & Calver, M.A., eds., The Winterborne Kingston borehole, Dorset: Report of the Institute of Geological Sciences 81/3, p. 91-96.

Knox, R.W.O.B., Morton, A.C., & Lott, G.K., 1982, Petrology of the Bridport Sands in the Winterborne Kingston borehole, Dorset, *in* Rhys, G.H., Lott, G.K., & Calver, M.A., eds., The Winterborne Kingston borehole, Dorset: Report of the Institute of Geological Sciences 81/3, p. 107-121.

Leithold, E.L., 1993, Preservation of laminated shale in ancient clinoforms; comparison to modern subaqueous deltas: Geology, v. 21, p. 359-362.

Leithold, E.L., 1994, Stratigraphical architecture at the muddy margin of the Cretaceous Western Interior Seaway, Southern Utah: Sedimentology, v. 41, p. 521-542.

Liu, J.P., Milliman, J.D., Gao, S., & Cheng, P., 2004, Holocene development of the Yellow River's subaqueous delta, North Yellow Sea: Marine Geology, v. 209, p. 45–67.

Liu, J.P., Li, A.C., Xu, K.H., Velozzi, D.M., Yang, Z.S., Milliman, J.D., & DeMaster, D.J., 2006, Sedimentary features of the Yangtze River-derived along-shelf clinoform deposit in the East China Sea: Continental Shelf Research, v. 26, p. 2141–2156.

MacEachern, J.A. & Bann, K.L., 2008, The role of ichnology in refining shallow marine facies models, *in* Hampson, G.J., Steel, R.J., Burgess, P.M., and Dalrymple, R.W., eds., Recent Advances in Models of Siliciclastic Shallow-Marine Stratigraphy: SEPM, Special Publication 90, p. 73-116.

MacEachern, J.A., Raychaudhuri, I., & Pemberton, S.G., 1992, Stratigraphic applications of the Glossifungites ichnofacies: delineating discontinuities in the rock record***, in*** Pemberton, S.G., ed., Applications of Ichnology to Petroleum Exploration; a core workshop: SEPM. Core Workshop 17, p. 169-198,

Macquaker, J.H.S. & Gawthorpe, R.L., 1993, Mudstone lithofacies in the Kimmeridge Clay Formation, Wessex Basin, southern England; implications for the origin and controls of the distribution of mudstones: Journal of Sedimentary Research, v. 63, p. 1129-1143.

Macquaker, J.H.S. & Howell, J.K., 1999, Small-scale (<5.0 m) vertical heterogeneity in mudstones: implications for high-resolution stratigraphy in siliciclastic mudstone successions: Journal of the Geological Society of London, v. 156, p. 105-112.

Macquaker, J.H.S., Bentley, S.J., & Bohacs, K.M., 2010, Wave-enhanced sediment gravity flows and mud dispersal across continental shelves: reappraising sediment transport processes operating in ancient mudstone successions: Geology, v. 38, p. 947-950.

Michels, K.H., Kudrass, H.R., Hübscher, C., Suckow, A., & Wiedicke, M., 1998, The submarine delta of the Ganges–Brahmaputra: cyclone-dominated sedimentation patterns: Marine Geology, v. 149, p. 133–154.

Milliman, J.D., & Meade, R.H., 1983, World-wide delivery of river sediment to the oceans: Journal of Geology, v. 91, p. 1-21.

Mitchell, N.C., Masselink, G., Huthnance, J.M., Fernández-Salas, L.M., & Lobo, J.A., 2012, Depth of modern coastal sand clinoforms: Journal of Sedimentary Research, v. 82, p. 469-481.

Morris, J.E., Hampson, G.J. & Johnson, H.D., 2006, A sequence stratigraphic model for an intensely bioturbated shallow-marine sandstone: the Bridport Sand Formation, Wessex Basin, UK: Sedimentology, v. 53, p. 1229-1263.

Morton, A. C. 1982. Heavy minerals from the sandstones of the Winterborne Kingston borehole, Dorset, *in* Rhys, G.H., Lott, G.K., & Calver, M.A., eds., The Winterborne Kingston borehole, Dorset: Report of the Institute of Geological Sciences 81/3, p. 143-148.

Ogg, J.G. & Hinnov, L.A., 2012, Jurassic, *in:* Gradstein, F.M., Ogg, J.G., Schmitz, M.D., & Ogg, G.M. (eds) *The Geologic Time Scale 2012*: Elsevier, Amsterdam, p. 731-791.

Patruno, S., Hampson, G.J., Jackson, C.A-L. & Dreyer, T., 2015a, Clinoform geometry, geomorphology, facies character and stratigraphic architecture of an ancient sand-rich subaqueous delta: Upper Jurassic Sognefjord Formation, Troll Field, offshore Norway: Sedimentology, v. 62, p. 350-388.

Patruno, S., Hampson, G.J. & Jackson, C.A-L., 2015b, Quantitative characterisation of deltaic and subaqueous clinoforms: Earth-Science Reviews, v. 142, p. 79-119.

Patruno, S., Hampson, G.J., Jackson, C.A-L. & Whipp, P.S., 2015c, Quantitative progradation dynamics and stratigraphic architecture of ancient shallow-marine clinoform sets: a new method and its application to the Upper Jurassic Sognefjord Formation, Troll Field, offshore Norway: Basin Research, v. 27, p. 412-452.

Penn, I.E., 1982, Middle Jurassic stratigraphy and correlation of the Winterborne Kingston borehole, *in* Rhys, G.H., Lott, G.K., & Calver, M.A., eds., The Winterborne Kingston borehole, Dorset: Report of the Institute of Geological Sciences 81/3, p. 53-76.

Pickering, K.T., 1995, Are enigmatic erosional sandy wave-like bedforms in Jurassic Bridport Sands, Dorset, due to standing waves?: Journal of the Geological Society of London, v. 152, p. 481-485.

Pirmez, C., Pratson, L.F., & Steckler, M.S., 1998, Clinoform development by advection-diffusion of suspended sediment: modeling and comparison to natural systems: Journal of Geophysical Research, v. 103, p. 24141–24157.

Plint, A.G., 2014, Mud dispersal across a Cretaceous prodelta: storm-generated, wave-enhanced sediment gravity flows inferred from mudstone microtexture and microfacies: Sedimentology, v. 61, p. 609-647.

Rhys, G.H., Lott, G.K., & Calver, M.A., 1982, Foreward to the Winterborne Kingston borehole report, *in* Rhys, G.H., Lott, G.K., & Calver, M.A., eds., The Winterborne Kingston borehole, Dorset: Report of the Institute of Geological Sciences 81/3, p. 1-18.

Rich, J.L., 1951, Three critical environments of deposition and criteria for recognition of rocks deposited in each of them: Geological Society of America, Bulletin, v. 62, p. 1-20.

Röhl, H.-J., Schmid-Röhl, A., Oschmann, W., Frimmel, A. & Schwark, L., 2001, The Posidonia Shale (Lower Toarcian) of SW-Germany: an oxygen-depleted ecosystem controlled by sea level and palaeoclimate: Palaeogeography, Palaeoclimatology, Palaeoecology, v. 165, p. 27-52.

Sadler, P.M., 1981, Sediment accumulation rates and the completeness of stratigraphic sections: Journal of Geology, v. 89, p. 569-584.

Sangree, J.B. & Widmier, R.M., 1977, Seismic stratigraphy and global changes in sea level, part 9: seismic interpretation of depositional facies, *in* Payton, C.E., ed., Seismic Stratigraphy - Applications to Hydrocarbon Exploration: American Association of Petroleum Geologists, Memoir 26, p. 165-184.

Savrda, C.E. & Bottjer, D.J., 1989: Trace-fossil model for reconstructing oxygenation histories of ancient marine bottom waters: application to Upper Cretaceous Niobrara Formation, Colorado: Palaeogeography, Palaeoclimatology, Palaeoecology, v. 74, p. 49-74.

Sultan, N., Cattaneo, A., Urgeles, R., Lee, H., Locat, J., Trincardi, F., Berne, S., Canals, M. & Lafuerza, S., 2008, A geomechanical approach for the genesis of sediment undulations on the Adriatic shelf: Geochemistry, Geophysics, and Geosystems, v. 9, Q04R03.

Swenson, J.B., Paola, C., Pratson, L., Voller, V.R. & Murray, A.B., 2005, Fluvial and marine controls on combined subaerial and subaqueous delta progradation: morphodynamic modeling of compound-clinoform development: Journal of Geophysical Research: Earth Surface, v. 110, F02013, 1-16.

Taylor, A.M. & Goldring, R., 1993, Description and analysis of bioturbation and ichnofabric: Journal of the Geological Society of London, v. 150, p. 141-148.

Vakarelov, B.K., Winker, C.D. & Bhattacharya, J.P., 2005, The missing mud belts of the ancient record: implications for sequence stratigraphy (abstract): AAPG, Annual Convention Program 14, p. A144.

Vigliotti, L., Verosub., K.L., Cattaneo, A., Trincardi, F., Asioli, A. & Piva, A., 2008, Palaeomagnetic and rock magnetic analysis of Holocene deposits from the Adriatic Sea: detecting and dating short-term fluctuations in sediment supply: The Holocene v. 18, p. 141-152.

TABLE AND FIGURE CAPTIONS

Table 1

Summary of sedimentary facies. Intensity of bioturbation is described using the bioturbation index of Taylor and Goldring (1993), and ichnofabrics are taken from Morris et al. (2006).

Figure 1

Schematic morphology in shoreline-perpendicular cross-section of deltaic compound clinoforms, which comprise a subaerial clinoform and a subaqueous clinoform separated by a broad subaqueous platform that is characterised by sediment bypass (e.g. Pirmez et al. 1998; Driscoll and Karner 1999; Swenson et al. 2005; Mitchell et al. 2012). The subaqueous clinoform typically extends for large distances (10s-100s km) out of the plane of cross-section, as a result of advective, shore-parallel sediment transport (Cattaneo et al. (2003). Such compound clinoform morphologies are common in modern tide- and wave-dominated deltas. Two compound clinoforms with a progradational architecture are sketched; note that the thickest sediment accumulations occur on the clinoform foresets.

Figure 2

(**A**) Map showing interpreted orientation, extent and distribution of subaqueous clinoform sets in the Down Cliff Clay Member (after Hampson et al., 2015). Jurassic extensional faults (after Hawkes et al., 1998) and the depositional limits of the Bridport Sand Formation in the subsurface Wessex Basin are shown (after Ainsworth et al., 1998; Hawkes et al., 1998). Inset map shows Toarcian palaeogeography, with landmasses shaded gray (redrawn from Röhl et al. 2001). (**B**) More detailed map of interpreted clinoform orientation, extent and distribution in subaqueous clinoform sets 3 and 4 of the Down Cliff Clay Member (Fig. 2A), based on apparent and true clinoform orientations observed in 2D and 3D seismic data (e.g. Figs. 4, 5) (Hampson et al., 2015). Subaqueous clinoforms defining clinoform-set boundaries are shown in green, and subaqueous clinoforms within sets are shown in orange.

Figure 3

(**A**) Tethyan ammonite zones and subzones of the Toarcian and early Aalenian strata that contain the Bridport Sand Formation and Down Cliff Clay Member in the Wessex Basin, showing interpolated absolute ages for the ammonite zones (Ogg and Hinnov, 2012; their Table 26.3). Selected subzone boundaries are labelled "T1" to "Aa3". (**B**) Chronostratigraphic summary of the Bridport Sand Formation and Down Cliff Clay Member in selected locations in the Wessex Basin; the Winterborne Kingston no. 1 well, the Wytch Farm Field, and the Dorset coastal cliff outcrops (Fig. 4A) (after Ivimey-Cook, 1982; Penn, 1982; Callomon and Cope, 1995; Hesselbo and Jenkyns, 1995; Ainsworth et al., 1998). The interpreted subaqueous clinoform sets of Hampson et al. (2015) are shown by triangles in the Down Cliff Clay Member for each location (cf. Fig. 2), as are thinner, stacked subaerial clinoform sets in the Bridport Sand Formation.

Figure 4

(**A**) Map showing the distribution of 2D and 3D seismic data used to map subaqueous clinoforms and clinoform sets in the Down Cliff Clay Member (Fig. 2B). The map locates the Winterborne Kingston no. 1 well and the 2D seismic line that intersects it (Fig. 5), the Wytch Farm Field (Fig. 4B-E), and the Dorset coastal cliff outcrops (Fig. 3B). (**B**-**E**) Seismic-stratigraphic and seismic-geomorphic relationships in the Down Cliff Clay Member and Bridport Sand Formation, as imaged in 3D seismic data from the "central terrace" area of the Wytch Farm Field (after Morris et al., 2006; Hampson et al., 2015) (Figs. 2B, 4A). (**B**) Uninterpreted and (**C**) interpreted timeslice, and (**D**) uninterpreted and (**E**) interpreted cross-section of lower to middle Jurassic strata. The timeslice is taken at 800 ms, over a window of 780-820 ms, and is annotated to show the position of wells, the oil-water contact (OWC), post-depositional faults (black) and mapped clinoform surfaces (orange, numbered 1, 2, 3, 4, 6 and 7 as labeled in Fig. 4C, E). The cross-section is annotated to show clinoforms arranged in two sets (clinoforms 3-5 in lower set and clinoforms 6-7 in upper set) each of which records progradation. Clinoform surfaces 1 and 2 can be traced contiguously between the two sets, implying an overall "compound clinoform" geometry (cf. Fig. 1). None of the wells contain core from the Down Cliff Clay Member.

Figure 5

Seismic-stratigraphic and seismic-geomorphic relationships in the Down Cliff Clay Member, Bridport Sand Formation and Inferior Oolite Group, as imaged in (**A**) uninterpreted and (**B**) interpreted section of regional 2D seismic line GC73-28 (Fig. 4A). The section is annotated to show clinoforms arranged in one set in the Down Cliff Clay Member, and at least two aggradationally-to-progradationally stacked sets in the Bridport Sand Formation. Subaerial and subaqueous clinoform-set boundaries in the Down Cliff Clay Member and Bridport Sand Formation, respectively, are shown in green, and subaerial and subaqueous clinoforms within sets are shown in orange.

Figure 6

Core log and selected wireline logs (gamma ray, GR; density, RHOB; neutron porosity, NPHI) through the Winterborne Kingston no. 1 well, illustrating the facies and facies associations in the succession (Table 1). Lithostratigraphic formations in the well are highlighted in the gamma ray track, while selected ammonite subzone boundaries (labelled "T1" to "T10", cf. Fig. 3) are indicated with a sequence stratigraphic interpretation (after Hesselbo and Jenkyns, 1998). See Figures 4A and 5 for well location and link to seismic-stratigraphic and seismic-geomorphic relationships.

Figure 7

Photographs illustrating facies characteristics (Table 1) in core from the Winterborne Kingston no. 1 well. (**A, B**) Sandy bioclastic limestones (facies 1) containing crinoids, ammonites (am), belemnites (be), bivalves (bi) and brachiopods (br). Nodular calcite cementation, highlighted by pale coloration, overprints the lower, coarse-grained part of depositional event beds that are variably bioturbated. (**C**) Fossiliferous claystones and siltstones (facies 2) containing ammonites (am) and belemnites (be). **(D, E**) Dark-colored, non- to highly bioturbated claystones and siltstones (facies 3) intercalated with pale-colored, nodular, calcareous claystones and siltstones (facies 4). Bioturbation is dominated by *Chondrites* (*Ch*). Variations in bed geometry and burrow thickness indicate significantly more compaction in non-calcareous claystones and siltstones. (**F)** Non- to highly bioturbated claystones and siltstones (facies 3). Highly bioturbated interval containing *Chondrites* (*Ch*) and *Thalassinoides* (*Th*) is overlain by sparsely bioturbated interval. (**G**) Moderately to completely bioturbated siltstones (facies

5), containing *Chondrites* (*Ch*), Planolites (*Pl*), and *Terebellina* (*sensu lato*) (*Te*). (**H, I, J, K, L, M, N**) Moderately to intensely bioturbated, sandy siltstones (facies 6), containing *Chondrites* (*Ch*), *Anconichnus* (*An*), *Teichichnus* (*T*), *Planolites* (*Pl*), *Asterosoma* (*As*), *Terebellina* (*sensu lato*) (*Te*), and escape traces (fugichnia, fu). Primary physical structures are preserved within thin, parallel-laminated sandstone beds with erosionally scoured based (Fig. J, K) and current-ripple cross-laminated sandstone lenses (Fig. 7L, M, N). (**O**) Chloritic siltstones (facies 8) containing phosphatic pebbles (pp) and belemnites (be). (**P**) Iron-stained, oolitic siltstones (facies 7). Photographs in Figure 7A-P are taken from 1116.3 m, 1115.6 m, 1117.5 m, 1107.5 m, 1105.8 m, 1086.9 m, 1076.6 m, 1076.8 m, 1018.4 m, 1042.8 m, 1052.3 m, 1059.4 m, 1046.1 m, 1023.8 m, 1016.0 m, and 1015.8 m, respectively (Fig. 6).

Figure 8

Model illustrating compound clinoform morphology, distribution of facies associations (Table 1), and sediment transport processes interpreted for the Bridport Sand Formation and Down Cliff Clay Member, based on seismic data (Figs. 4, 5) and core data from the Winterborne Kingston no. 1 well (Figs. 6, 7) (partly after Morris et al. 2006; Hampson et al. 2015). The upper part of the Bridport Sand Formation corresponds to the subaerial deltaic clinoform (labelled “shoreface”), and the Down Cliff Clay Member corresponds to the subaqueous deltaic clinoform (labelled “facies associations B, C and D”).

Figure 9

Subaqueous clinoform geometry and vertical sediment accumulation rates in the clinoform foresets of (**A**) the modern Ganges-Brahmaputra Delta (Michels et al. 1998), (**B**) modern western Adriatic shelf (Cattaneo et al. 2003, 2007), and (**C**) the Toarcian Down Cliff Clay Member (this paper). Note that vertical sediment accumulation rates are shown at different scales in each of the three examples, and that clinoform geometry and vertical sediment accumulation rate do not take decompaction into account for the Down Cliff Clay Member.

Facies	Lithology and Sedimentary Structures	Ichnology	Thickness	Interpretation
1: sandy bioclastic limestones	Variably laminated and variably bioturbated bioclastic grainstone composed of thin (5-40 cm), erosionally based, upward-fining beds. Some bed boundaries are modified by nodular calcite cementation. Abundant bioclasts (notably crinoid ossicles, but also variably fragmented ammonites, belemnites, brachiopods, bivalves) and fine-grained quartz sand grains.	BI: 1-6 (*Terebellina*, *Thalassinoides*, *Planolites*, *Palaeophycus*, small *Arenicolites*). Unlined, passively filled *Thalassinoides* at erosional bed boundaries.	0.5-2.5 m	Siliciclastic sediment starvation and episodic erosional reworking. Abundant benthic and nektonic body fossils and diverse trace fossil assemblage imply deposition in a shallow, fully marine environment, potentially above fairweather wave base.
2: fossiliferous claystones and siltstones	Variably laminated and variably bioturbated claystones and siltstones. Abundant body fossils (ammonites, belemnites, brachiopods, bivalves).	BI: 3-4 (*Chondrites*).	0.1-0.2 m	Condensed deposition of clay and silt from suspension, below effective storm wave base. Monospecific trace fossil assemblage implies intermittent oxygenation of bottom waters.
3: non- to highly bioturbated claystones and siltstones	Variably bioturbated claystones and siltstones. Parallel laminated where not overprinted by bioturbation. Sparse, partly fragmented body fossils (ammonites, belemnites, brachiopods, bivalves).	BI: 0-4 (*Chondrites*, *Planolites*, *Thalassinoides*).	0.0-5.0 m	Deposition of clay and silt from suspension and/or intermittent sediment gravity flows and tractional currents. Restricted trace fossil assemblage implies intermittent and/or poor oxygenation of bottom waters.
4: nodular, calcareous claystones and siltstones	Bioturbated, calcareous claystones and siltstones. Bed boundaries are modified by nodular calcite cementation and associated differential compaction. Sparse to abundant body fossils (ammonites, belemnites, brachiopods, bivalves).	BI: 2-4 (*Chondrites*, *Planolites*, *Thalassinoides*).	0.0-0.2 m	Local diffusion of bioclast-sourced calcium carbonate and related calcite cementation during early diagenesis, prior to deep burial. Restricted trace fossil assemblage implies intermittently poor oxygenation of bottom waters.
5: moderately to completely bioturbated siltstones	Bioturbated siltstones with rare, thin (<1 cm), erosionally based siltstone and very fine-grained sandstone beds. Parallel laminated where not overprinted by bioturbation. Very sparse body fossils (belemnites).	BI: 3-6 by Helminthopsis and Anchonichnus motting ichnofabrics of Morris et al. (2006): *Terebellina* (*sensu lato*), *Helminthopsis*, small *Teichichnus*, *Chondrites*, *Planolites*, *Anconichnus*.	0.0-8.4 m	Deposition of predominantly silt from intermittent sediment gravity flows and tractional currents, with a minor contribution from suspension, above effective storm wave base and below fairweather wave base.
6: moderately to intensely bioturbated, sandy siltstones	Bioturbated sandy siltstones with thin (<1 cm), erosionally based, very fine-grained sandstone beds containing variably preserved parallel lamination and current-ripple cross-lamination. Body fossils are absent.	BI: 3-5 by Terebellina 1 and Anchonichnus motting ichnofabrics of Morris et al. (2006): *Terebellina* (*sensu lato*), *Helminthopsis*, *Zoophycos*, *Asterosoma*, small *Teichichnus*, *Chondrites*, *Planolites*, *Anconichnus*.	0.1-4.5 m	Deposition of silt and very fine sand from intermittent sediment gravity flows and tractional currents, with a minor proportion of silt deposited from suspension, above effective storm wave base and below fairweather wave base.
7: iron-stained, oolitic siltstones	Red siltstones and sandy siltstones containing abundant matrix-supported, iron-stained and phosphatic ooids. Abundant fragmented and	BI: 4 by Terebellina 1 ichnofabric of Morris et al. (2006): *Terebellina*, *Helminthopsis*, *Zoophycos*, *Asterosoma*,	0.3 m	Deposition of transported clasts that record extended physical reworking and siliciclastic sediment starvation.

	abraded body fossils (ammonites, belemnites, bivalves, gastropods).	small *Teichichnus*, *Chondrites*, *Planolites*.		
8: chloritic siltstones	Structureless green siltstone containing phosphatic pebbles and rare, iron-stained, fragmented body fossils (ammonites, belemnites).	BI: 2 (*Chondrites*).	0.2 m	Deposition of transported clasts that record extended physical reworking and siliciclastic sediment starvation. Monospecific trace fossil assemblage implies intermittently poor oxygenation of bottom waters.

Table 1
Summary of sedimentary facies. Intensity of bioturbation is described using the bioturbation index of Taylor and Goldring (1993), and ichnofabrics are taken from Morris et al. (2006).

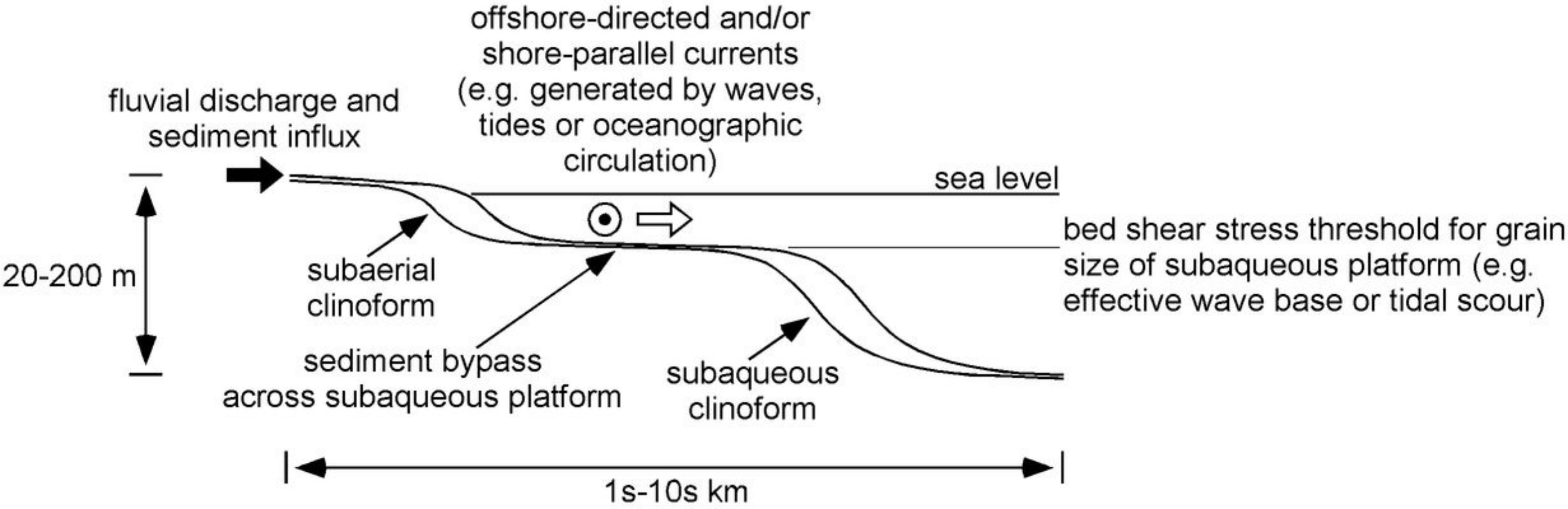
offshore-directed and/or
shore-parallel currents
(e.g. generated by waves,
tides or oceanographic
circulation)
fluvial discharge and
sediment influx
sea level
bed shear stress threshold for grain
size of subaqueous platform (e.g.
effective wave base or tidal scour)
20-200 m
subaerial
clinoform
sediment bypass
across subaqueous platform
subaqueous
clinoform
1s-10s km

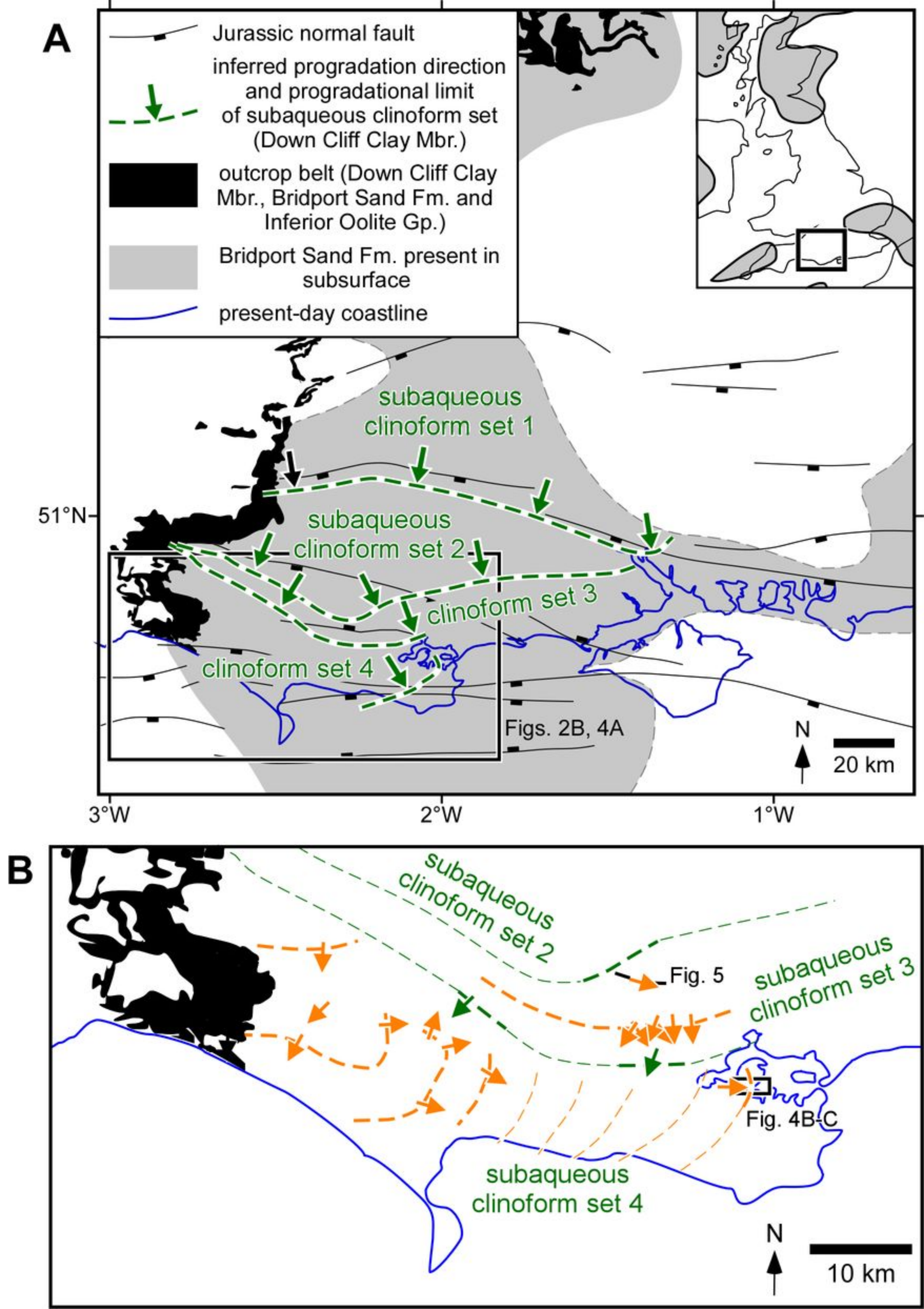
A
Jurassic normal fault
inferred progradation direction and progradational limit of subaqueous clinoform set (Down Cliff Clay Mbr.)
outcrop belt (Down Cliff Clay Mbr., Bridport Sand Fm. and Inferior Oolite Gp.)
Bridport Sand Fm. present in subsurface
present-day coastline
subaqueous clinoform set 1
subaqueous clinoform set 2
clinoform set 3
clinoform set 4
Figs. 2B, 4A
51°N
3°W
2°W
1°W
N
20 km
B
subaqueous clinoform set 2
subaqueous clinoform set 3
Fig. 5
Fig. 4B-C
subaqueous clinoform set 4
N
10 km

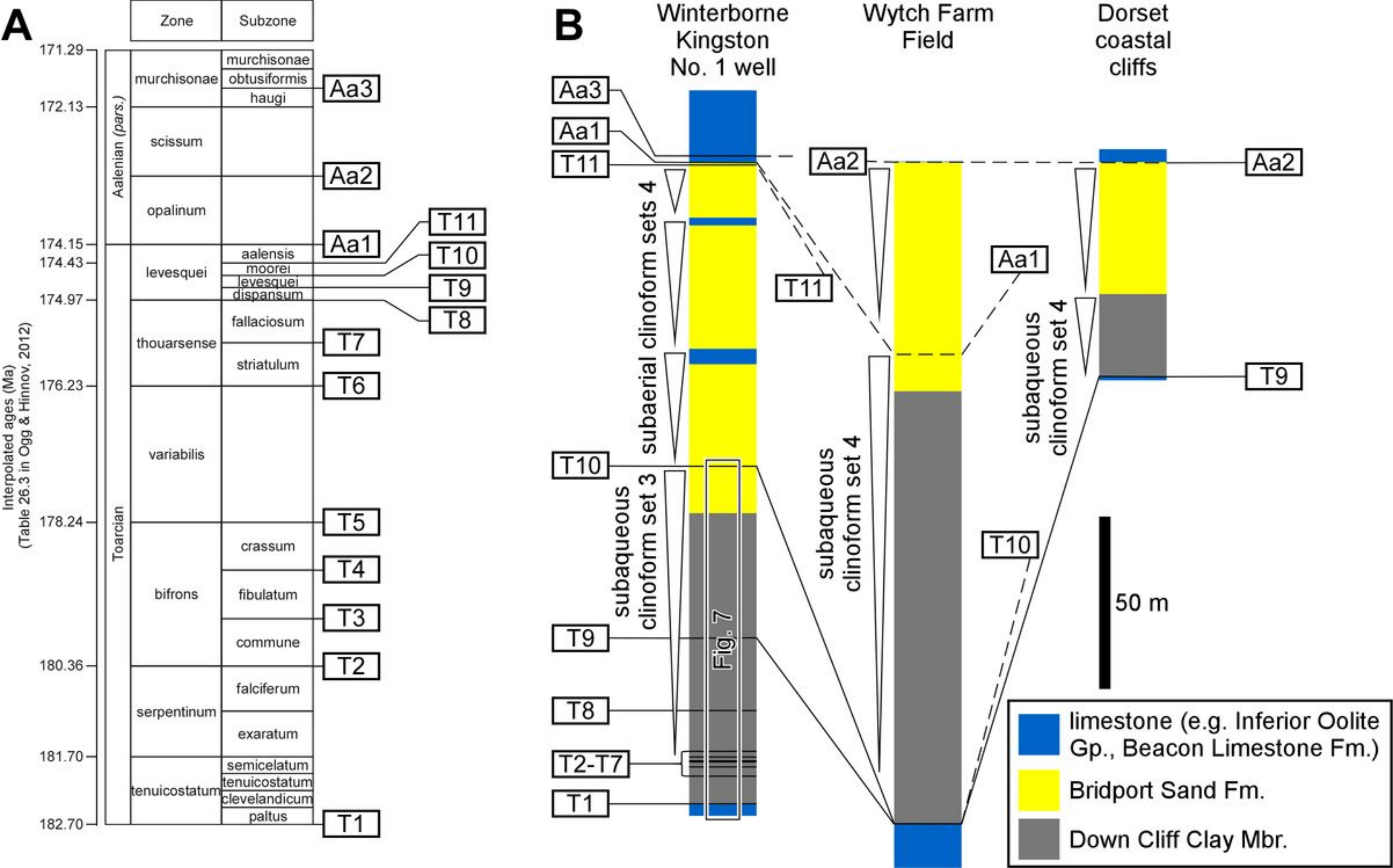

A
Zone
Subzone
Interpolated ages (Ma) (Table 26.3 in Ogg & Hinnov, 2012)
171.29
172.13
174.15
174.43
174.97
176.23
178.24
180.36
181.70
182.70
Aalenian (pars.)
Toarcian
murchisonae
scissum
opalinum
levesquei
thouarsense
variabilis
bifrons
serpentinum
tenuicostatum
murchisonae
obtusiformis
haugi
aalensis
moorei
levesquei
dispansum
fallaciosum
striatulum
crassum
fibulatum
commune
falciferum
exaratum
semicelatum
tenuicostatum
clevelandicum
paltus
Aa3
Aa2
Aa1
T11
T10
T9
T8
T7
T6
T5
T4
T3
T2
T1
B
Winterborne Kingston No. 1 well
Wytch Farm Field
Dorset coastal cliffs
Aa3
Aa1
T11
Aa2
Aa1
T11
Aa2
subaerial clinoform sets 4
subaqueous clinoform set 3
subaqueous clinoform set 4
subaqueous clinoform set 4
T10
T9
T8
T2-T7
T1
T10
T9
Fig. 7
50 m
limestone (e.g. Inferior Oolite Gp., Beacon Limestone Fm.)
Bridport Sand Fm.
Down Cliff Clay Mbr.

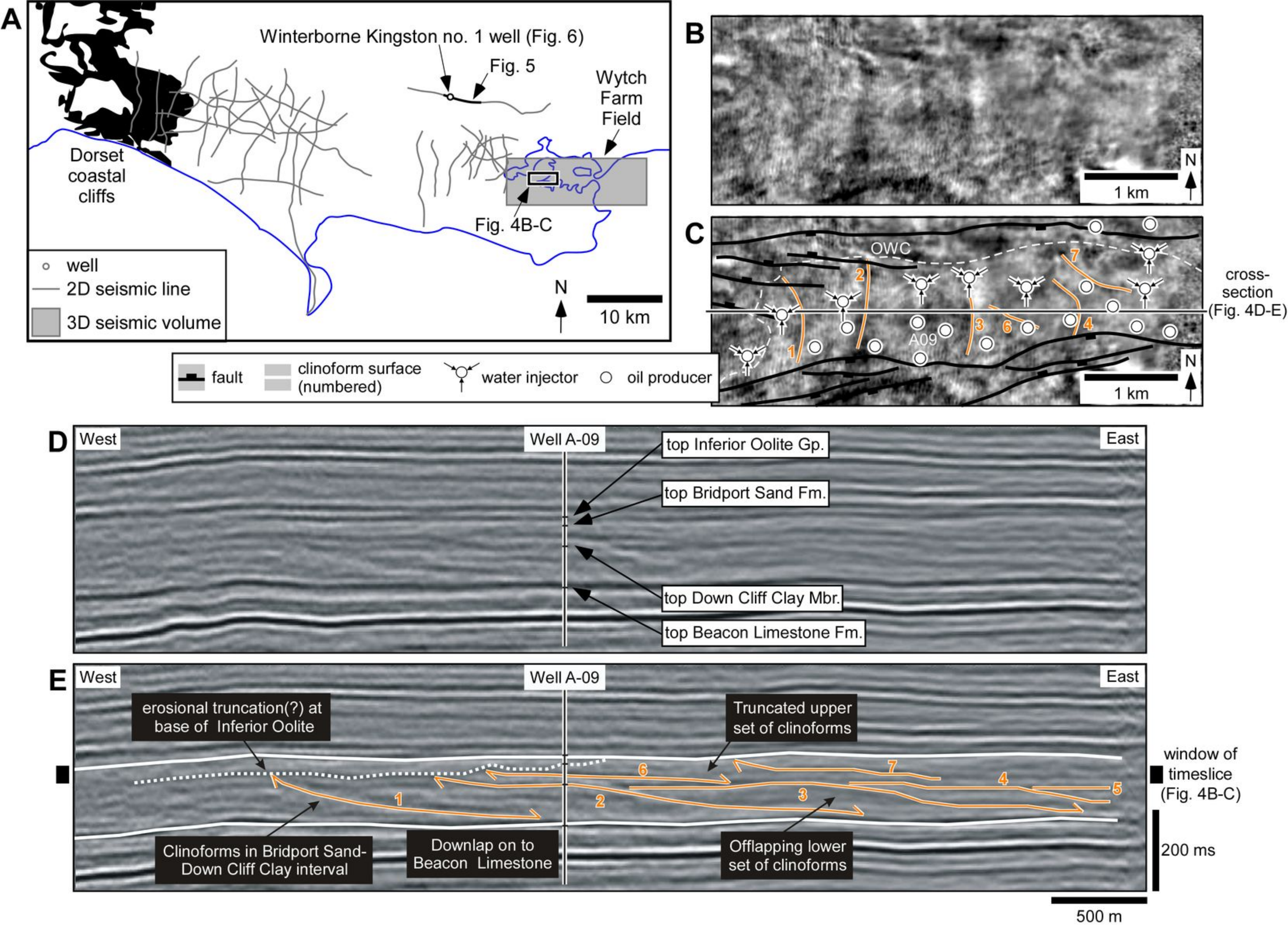

A
Winterborne Kingston no. 1 well (Fig. 6)
Fig. 5
Wytch Farm Field
Dorset coastal cliffs
Fig. 4B-C
well
2D seismic line
3D seismic volume
N
10 km
B
1 km
C
OWC
A09
1
2
3
4
6
7
cross-section (Fig. 4D-E)
fault
clinoform surface (numbered)
water injector
oil producer
D
West
Well A-09
East
top Inferior Oolite Gp.
top Bridport Sand Fm.
top Down Cliff Clay Mbr.
top Beacon Limestone Fm.
E
erosional truncation(?) at base of Inferior Oolite
Truncated upper set of clinoforms
Clinoforms in Bridport Sand-Down Cliff Clay interval
Downlap on to Beacon Limestone
Offlapping lower set of clinoforms
5
window of timeslice (Fig. 4B-C)
200 ms
500 m

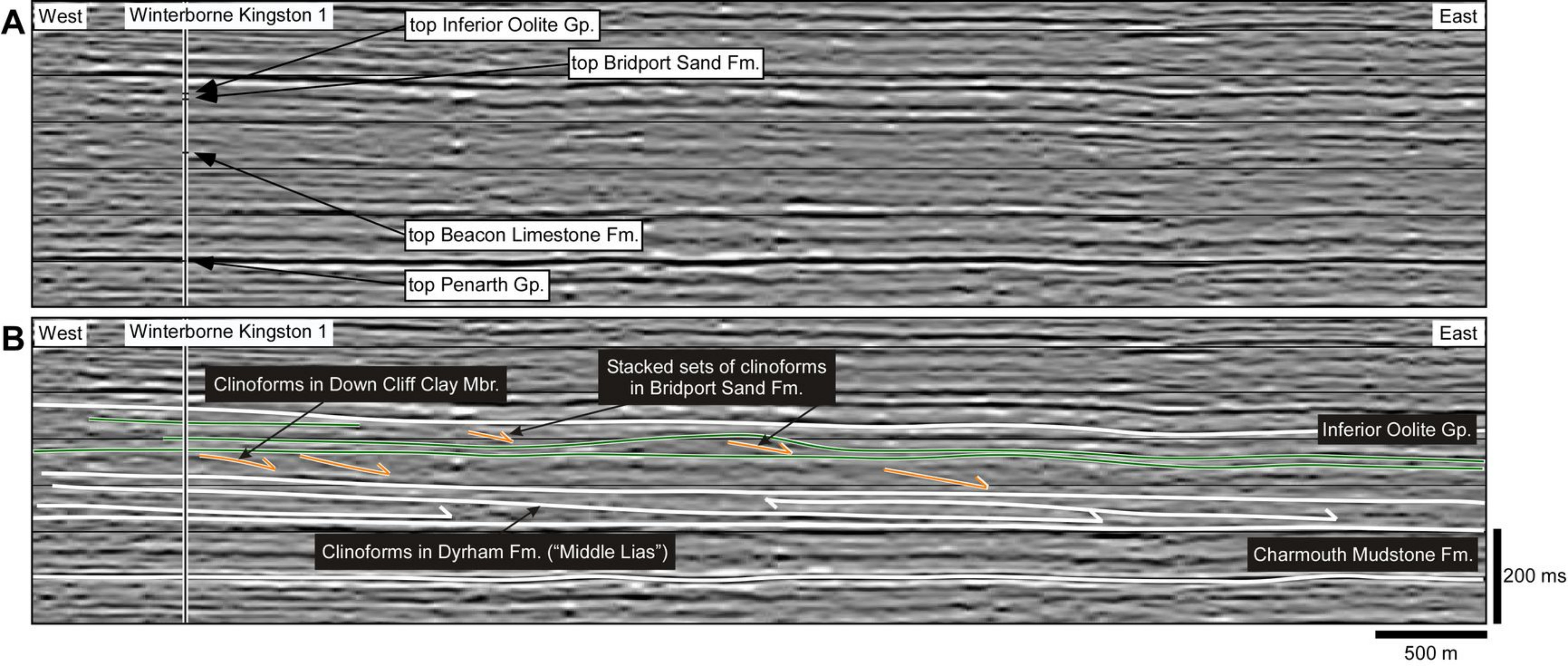
A
West
Winterborne Kingston 1
East
top Inferior Oolite Gp.
top Bridport Sand Fm.
top Beacon Limestone Fm.
top Penarth Gp.
B
West
Winterborne Kingston 1
East
Clinoforms in Down Cliff Clay Mbr.
Stacked sets of clinoforms in Bridport Sand Fm.
Inferior Oolite Gp.
Clinoforms in Dyrham Fm. ("Middle Lias")
Charmouth Mudstone Fm.
200 ms
500 m

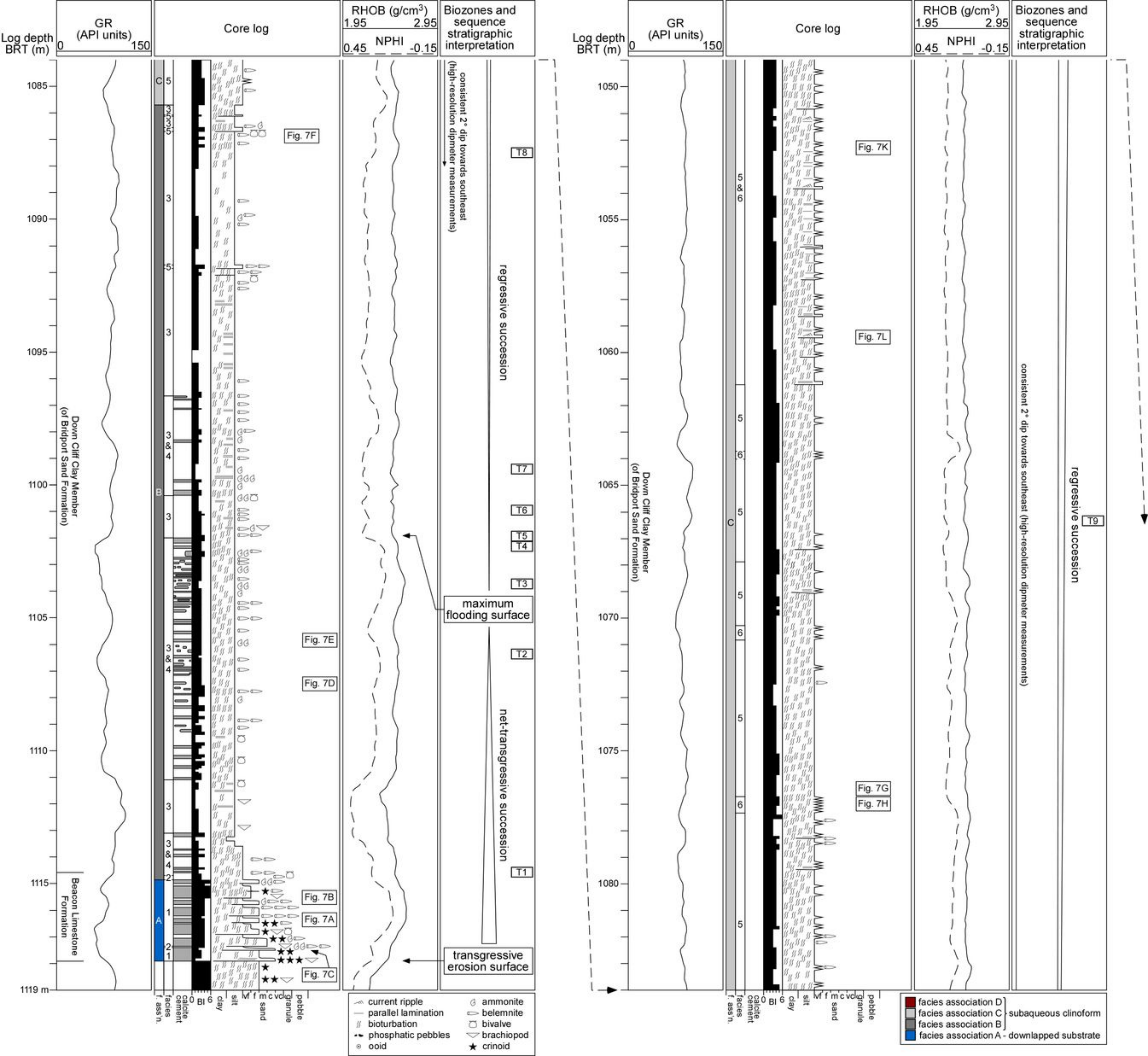
Log depth BRT (m)
GR (API units)
0
150
Core log
RHOB (g/cm^3)
1.95
2.95
NPHI
0.45
-0.15
Biozones and sequence stratigraphic interpretation
Down Cliff Clay Member (of Bridport Sand Formation)
Beacon Limestone Formation
consistent 2° dip towards southeast (high-resolution dipmeter measurements)
regressive succession
net-transgressive succession
maximum flooding surface
transgressive erosion surface
T1
T2
T3
T4
T5
T6
T7
T8
T9
Fig. 7A
Fig. 7B
Fig. 7C
Fig. 7D
Fig. 7E
Fig. 7F
Fig. 7G
Fig. 7H
Fig. 7K
Fig. 7L
f. ass'n.
facies
calcite cement
BI
clay
silt
sand
vf f m c vc
granule
pebble
1085
1090
1095
1100
1105
1110
1115
1119 m
1050
1055
1060
1065
1070
1075
1080
current ripple
parallel lamination
bioturbation
phosphatic pebbles
ooid
ammonite
belemnite
bivalve
brachiopod
crinoid
facies association D
facies association C
facies association B
facies association A - downlapped substrate
subaqueous clinoform

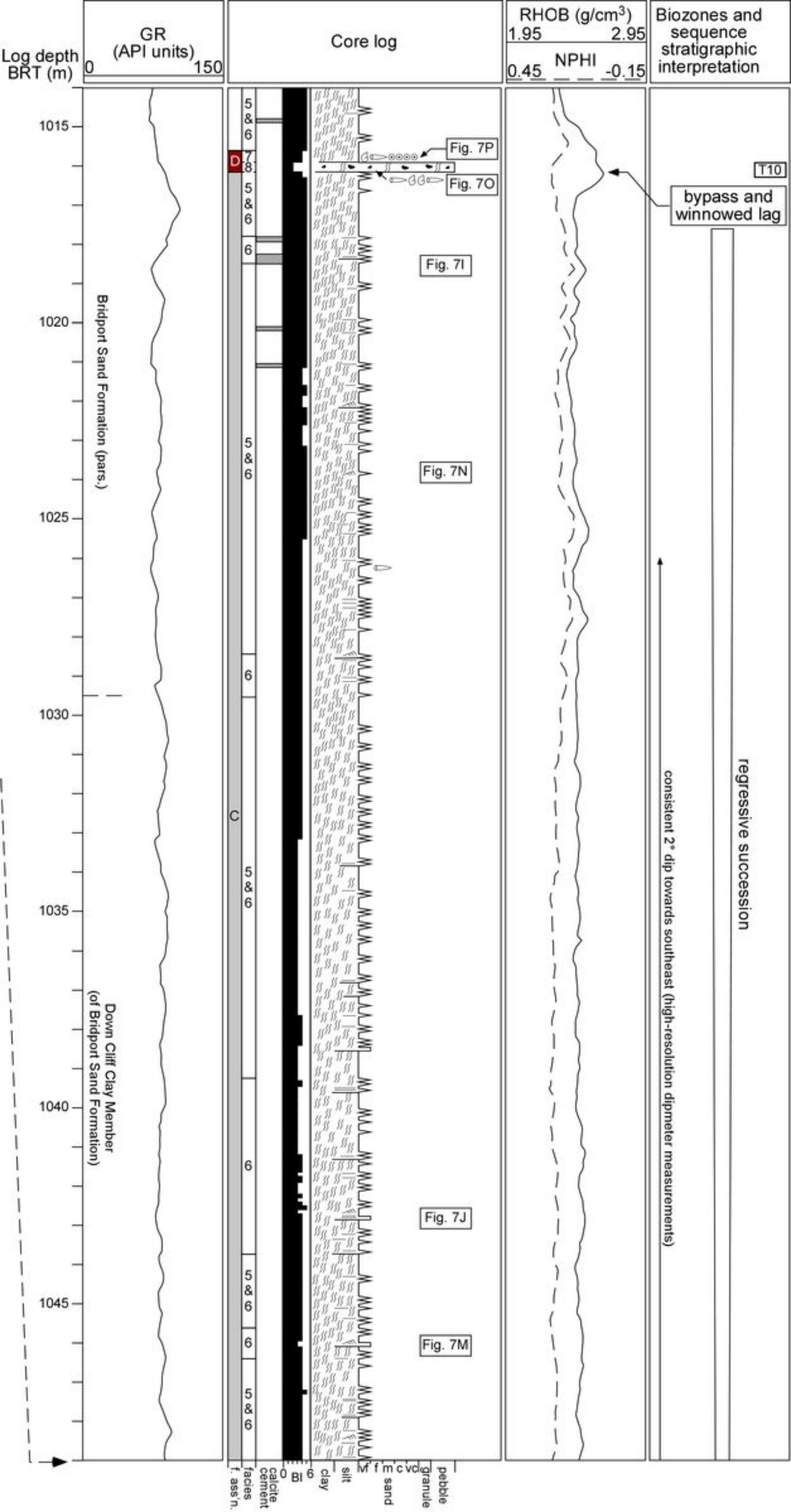

Log depth BRT (m)
GR (API units)
0
150
Core log
RHOB (g/cm³)
1.95
2.95
NPHI
0.45
-0.15
Biozones and sequence stratigraphic interpretation
1015
1020
1025
1030
1035
1040
1045
Bridport Sand Formation (pars.)
Down Cliff Clay Member (of Bridport Sand Formation)
D
C
5 & 6
7
8
6
Fig. 7P
Fig. 7O
Fig. 7I
Fig. 7N
Fig. 7J
Fig. 7M
T10
bypass and winnowed lag
consistent 2° dip towards southeast (high-resolution dipmeter measurements)
regressive succession
f. ass'n.
facies
calcite cement
0
BI
6
clay
silt
vf
f
m
c
vc
sand
granule
pebble

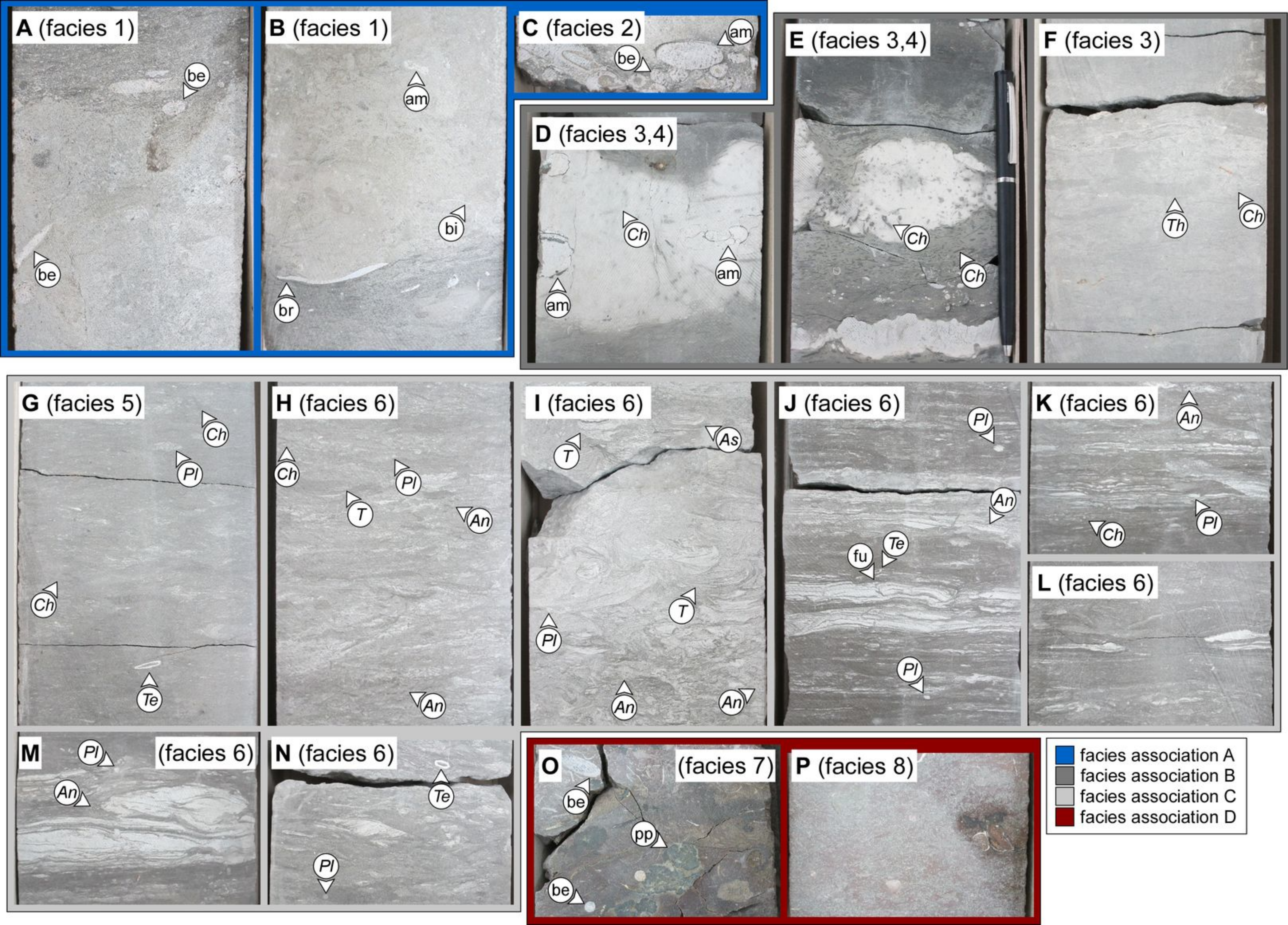
A (facies 1)
be
be
B (facies 1)
am
bi
br
C (facies 2)
am
be
D (facies 3,4)
Ch
am
am
E (facies 3,4)
Ch
Ch
F (facies 3)
Th
Ch
G (facies 5)
Ch
Pl
Ch
Te
H (facies 6)
Ch
Pl
T
An
An
I (facies 6)
T
As
T
Pl
An
An
J (facies 6)
Pl
An
fu
Te
Pl
K (facies 6)
An
Ch
Pl
L (facies 6)
M
(facies 6)
Pl
An
N (facies 6)
Te
Pl
O
(facies 7)
be
pp
be
P (facies 8)
facies association A
facies association B
facies association C
facies association D

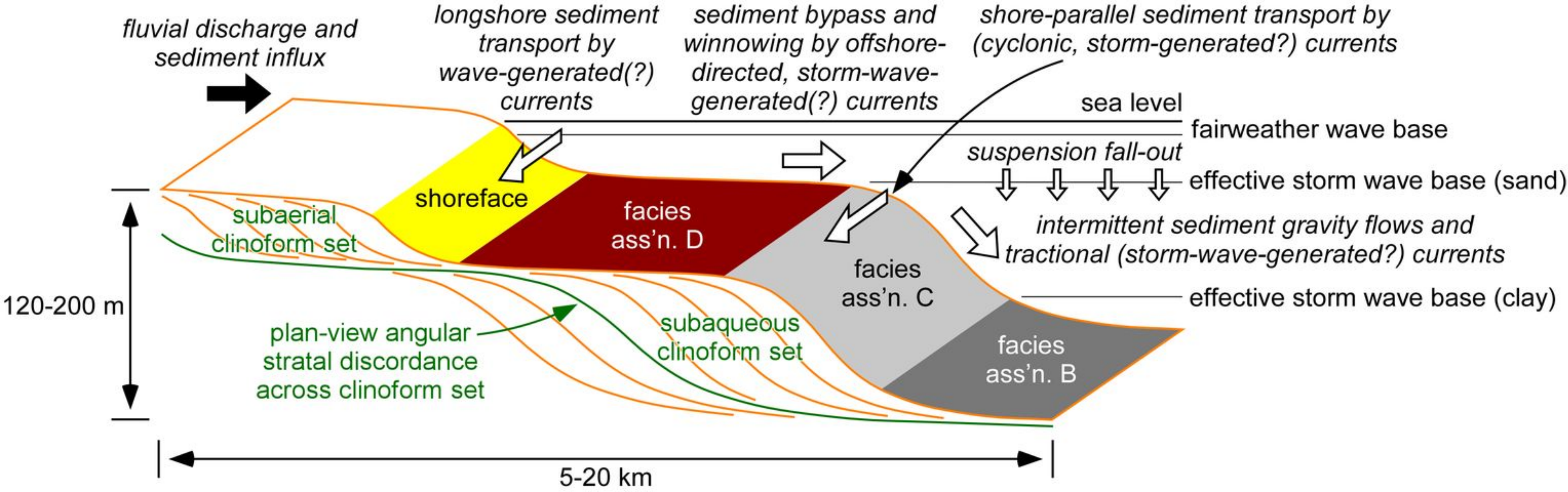
fluvial discharge and sediment influx
longshore sediment transport by wave-generated(?) currents
sediment bypass and winnowing by offshore-directed, storm-wave-generated(?) currents
shore-parallel sediment transport by (cyclonic, storm-generated?) currents
sea level
fairweather wave base
suspension fall-out
effective storm wave base (sand)
intermittent sediment gravity flows and tractional (storm-wave-generated?) currents
effective storm wave base (clay)
shoreface
facies ass'n. D
facies ass'n. C
facies ass'n. B
subaerial clinoform set
subaqueous clinoform set
plan-view angular stratal discordance across clinoform set
120-200 m
5-20 km

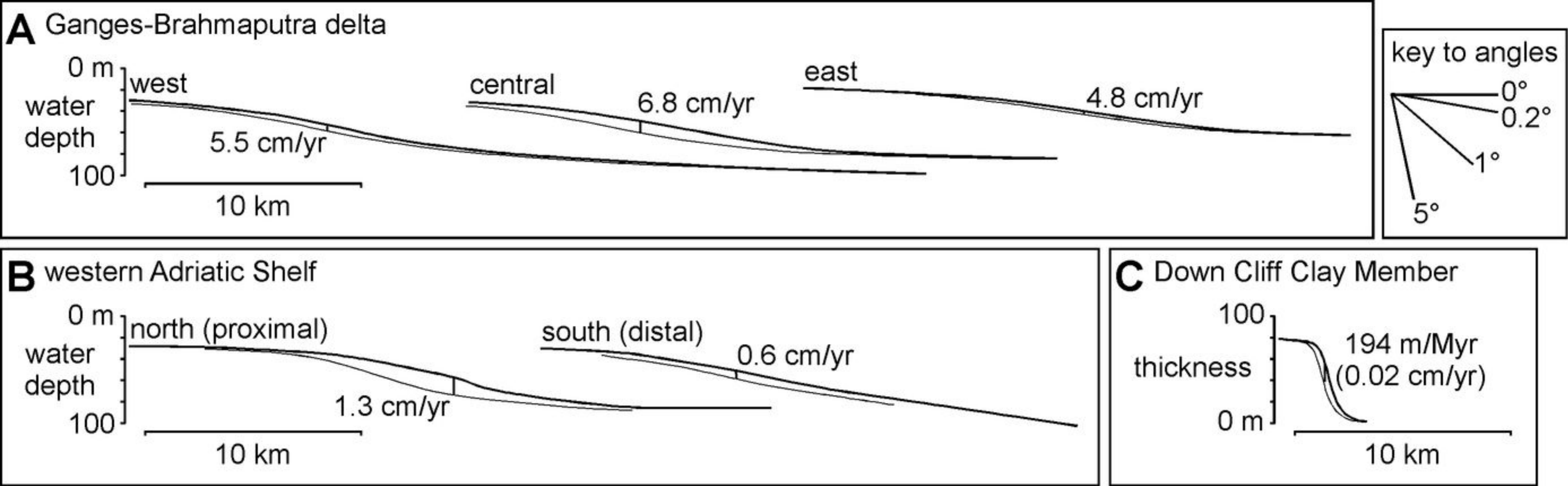
A Ganges-Brahmaputra delta
0 m
water depth
100
10 km
west
5.5 cm/yr
central
6.8 cm/yr
east
4.8 cm/yr
key to angles
0°
0.2°
1°
5°
B western Adriatic Shelf
0 m
water depth
100
10 km
north (proximal)
1.3 cm/yr
south (distal)
0.6 cm/yr
C Down Cliff Clay Member
100
thickness
0 m
10 km
194 m/Myr
(0.02 cm/yr)